

AN ABSTRACT OF THE THESIS OF

Dennis Paul Sandoz for the Master of Science in Chemistry (Analytical)
(Name) (Degree) (Major)

Date thesis is presented July 25, 1966

Title STUDIES OF ELECTRODE PROCESSES WITH VOLTAGE
SCANNING COULOMETRY

Abstract approved

Redacted for Privacy

(Major professor)

Voltage scanning coulometry was used to study the effects of electrode surfaces and metals on the electrochemistry of the ferric-ferrous couple and the silver ion-silver metal couple. The analytical technique called voltage scanning coulometry is very similar to controlled potential coulometry. The main difference is that in voltage scanning coulometry the potential of the working electrode is scanned through a voltage range rather than remaining at a constant potential.

The equations for voltage scanning coulometry were verified for the ferric-ferrous couple and silver deposition on a gold electrode. Indirect evidence is presented relating the activity of the silver deposit to the fraction of the electrode surface covered by the deposit. Evidence is presented showing the presence of both gold and platinum oxides on the surface of the electrodes.

Electrode treatments and their effects on the use of electrodes is thoroughly evaluated in terms of the electrochemical systems

studied here. Evidence is presented showing that the ferric-ferrous couple is catalyzed by a ceric treated electrode surface. The activity of a silver deposit on a ceric treated surface is found to be much greater than its activity on a crystalline surface. Qualitative evidence verifying the potential energy calculations for silver deposition at various surfaces is presented, also.

The effective to geometric surface area ratio for a crystalline gold electrode is found to be 2.3 for silver deposition. The deposition of the first monolayer of silver on a crystalline gold surface is found to occur at lattice sites with three different adsorption energies.

STUDIES OF ELECTRODE PROCESSES WITH
VOLTAGE SCANNING COULOMETRY

by

DENNIS PAUL SANDOZ

A THESIS

submitted to

OREGON STATE UNIVERSITY

in partial fulfillment of
the requirements for the
degree of

MASTER OF SCIENCE

June 1967

APPROVED:

Redacted for Privacy

Professor of Chemistry
In Charge of Major

Redacted for Privacy

Chairman, Department of Chemistry

Redacted for Privacy

Dean of Graduate School

Date thesis is presented July 25, 1966

Typed by Opal Grossnicklaus

ACKNOWLEDGEMENTS

I wish to take this opportunity to acknowledge the many persons who assisted me in this work: Dr. Richard M. Peekema for providing the original ideas and for guiding this work in its early stages; Dr. Harry Freund for guiding this work in its later stages and for assisting me in the preparation of this thesis; my wife, Sharon, for her help and understanding, without which this study would not have been completed.

TABLE OF CONTENTS

I. INTRODUCTION	1
II. THEORETICAL	2
III. EXPERIMENTAL	13
Cell Design	13
Instrumentation	17
Procedure	20
IV. RESULTS AND INTERPRETATION OF DATA	22
Ferric-Ferrous Couple	22
Electrode Treatments	32
Silver Deposition	39
Iodide-Iodine Couple	66
V. SUMMARY	69
BIBLIOGRAPHY	71

LIST OF FIGURES

<u>Figure</u>	<u>Page</u>
1. A plot of the Nernst equation.	5
2. Theoretical and experimental $\Delta Q/\Delta E$ plot.	6
3. Experimental and theoretical current-voltage plots for iron.	7
4. Cell I.	14
5. Cell II.	15
6. Block diagram of the voltage scanning coulometer.	18
7. A plot of indicator electrode potential versus working electrode potential I.	24
8. A plot of indicator electrode potential versus working electrode potential II.	25
9. Current versus potential of indicating electrode.	26
10. Experimental current-voltage plot for iron.	27
11. Hysteresis curve.	30
12. Reduction scans of the ceric treated platinum electrode.	36
13. Reduction scans of the ceric treated gold electrode.	37
14. Silver deposition on the crystalline gold surface.	41
15. Deposition of silver on the ceric treated gold electrode.	47
16. Deposition of silver on the gold electrode.	50
17. Stripping scans of silver from the crystalline gold surface.	53

LIST OF FIGURES (CONTINUED)

<u>Figure</u>	<u>Page</u>
18. Theoretical and experimental silver stripping curves at the ceric treated gold surface.	56
19. Stripping scans of silver from the ceric treated gold surface.	58
20. Deposition and stripping of silver at the crystalline gold surface.	60
21. Deposition and stripping of silver at the ceric treated gold surface.	61
22. Deposition and stripping of silver at the ceric treated platinum electrode.	64
23. Deposition and stripping of silver at the crystalline platinum surface.	65
24. Oxidation and reduction scans of iodine at the platinum electrode.	67

LIST OF TABLE

<u>Table</u>	<u>Page</u>
1. Polarization of the working electrode.	32

STUDIES OF ELECTRODE PROCESSES WITH VOLTAGE SCANNING COULOMETRY

I. INTRODUCTION

Voltage scanning coulometry was used to study the effects of electrode surfaces and metals on the electrochemistry of the ferric-ferrous couple and the silver ion-silver metal couple. The effects of the electrode surfaces and metals on the electrochemical systems studied were related to the mechanism of their respective electrode reactions. These electrochemical systems were also used to check the equations derived for voltage scanning coulometry.

Voltage scanning coulometry is a hybrid of controlled potential coulometry and polarography. Normal controlled potential coulometric cells are used in this work. As the name, voltage scanning coulometry, implies, the potential of the working electrode is slowly scanned through a desired potential range. Several references are included here that may be consulted for background information on controlled potential coulometry and its associated equipment (4; 15, p. 321; 18, p. 450; 22, p. 1-5; 29, p. 544).

II. THEORETICAL

To derive the equations presented in this section, a hypothetical solution containing one reducible species will be assumed. Both the oxidized and reduced forms are assumed to be present as ions in solution. It shall also be assumed that the half-reaction considered here is reversible. The Stockholm Convention, with regard to electrochemical potentials, will apply.

The equations below were derived by Peekema (22, p. 5-17) and the following is a brief presentation of his work.

The potential of an inert electrode in an aqueous solution can be described by the following form of the Nernst equation:

$$E = E^{\circ} + \frac{RT}{nF} \ln \frac{A_{\text{ox}}}{A_{\text{red}}}, \quad (1)$$

where E° is the potential of a cell consisting of the half-reaction considered here and the normal hydrogen electrode; and A_{ox} and A_{red} are the activities of the oxidized and the reduced species respectively.

Replacing the activities in Equation 1 with the product of their activity coefficients and concentrations, and absorbing the activity coefficients into $E^{\circ'}$, results in an expression which is easily simplified.

Since the volume of the solution for both the oxidized and reduced species is the same, it is cancelled from the above expression, yielding

$$E = E^{O'} + \frac{RT}{nF} \ln \frac{x}{y}, \quad (2)$$

where x is the number of moles of oxidized species and y is the number of moles of reduced species, with

$$E^{O'} = E^O + \frac{RT}{nF} \ln \frac{f_{ox}}{f_{red}}. \quad (3)$$

The symbols f_{ox} and f_{red} represent the activity coefficients of the oxidized and reduced species, respectively, which are considered constant throughout an experiment. The symbol m is used to represent the total number of moles of electroizable material and it is equal to the sum of x and y . The number of coulombs passed during an electrolysis, Q , is defined by the following equation, assuming we start out with the electrochemically active species in its oxidized form

$$Q = nFy = nF(m-x). \quad (4)$$

Solving for x and y in Equation 4 and substituting into Equation 2 yields

$$E = E^{O'} + \frac{RT}{nF} \ln \frac{Q_m - Q}{Q}. \quad (5)$$

The maximum value of Q is represented by Q_m and is defined by

$Q_m = nFm$. A plot of Equation 5 is shown in Figure 1.

To obtain dQ/dE for an electrochemical system, with both oxidized and reduced species present as ions in solution, Equation 5 can be differentiated yielding

$$\frac{-dQ}{dE} = \frac{nF}{RT} \cdot \frac{Q(Q_m - Q)}{Q_m} \quad (6)$$

Solving Equation 5 for Q and substituting for Q in Equation 6 yields

$$\frac{-dQ}{dE} = \frac{nFQ_m}{RT} \cdot \frac{P}{(1+P)^2} \quad (7)$$

with $P = \exp\left[\frac{nF}{RT} (E - E^{0'})\right]$. It shall be noted that the derivatives included in this thesis are partial derivatives with temperature and pressure considered constant.

Equation 7 can be further simplified yielding

$$-i = \frac{n^2 F^2 m}{RT} \cdot \frac{P}{(1+P)^2} \cdot (\text{voltage scan rate}). \quad (8)$$

A plot of Equation 7 is shown with an experimental curve in Figure 2. Shown in Figure 3, along with several experimental curves, is a plot of Equation 8.

From the shape of the theoretical curve in Figure 2, it can be seen that the maximum value for dQ/dE should occur at $E^{0'}$. The second derivative of Equation 6 is represented by Equation 9. By

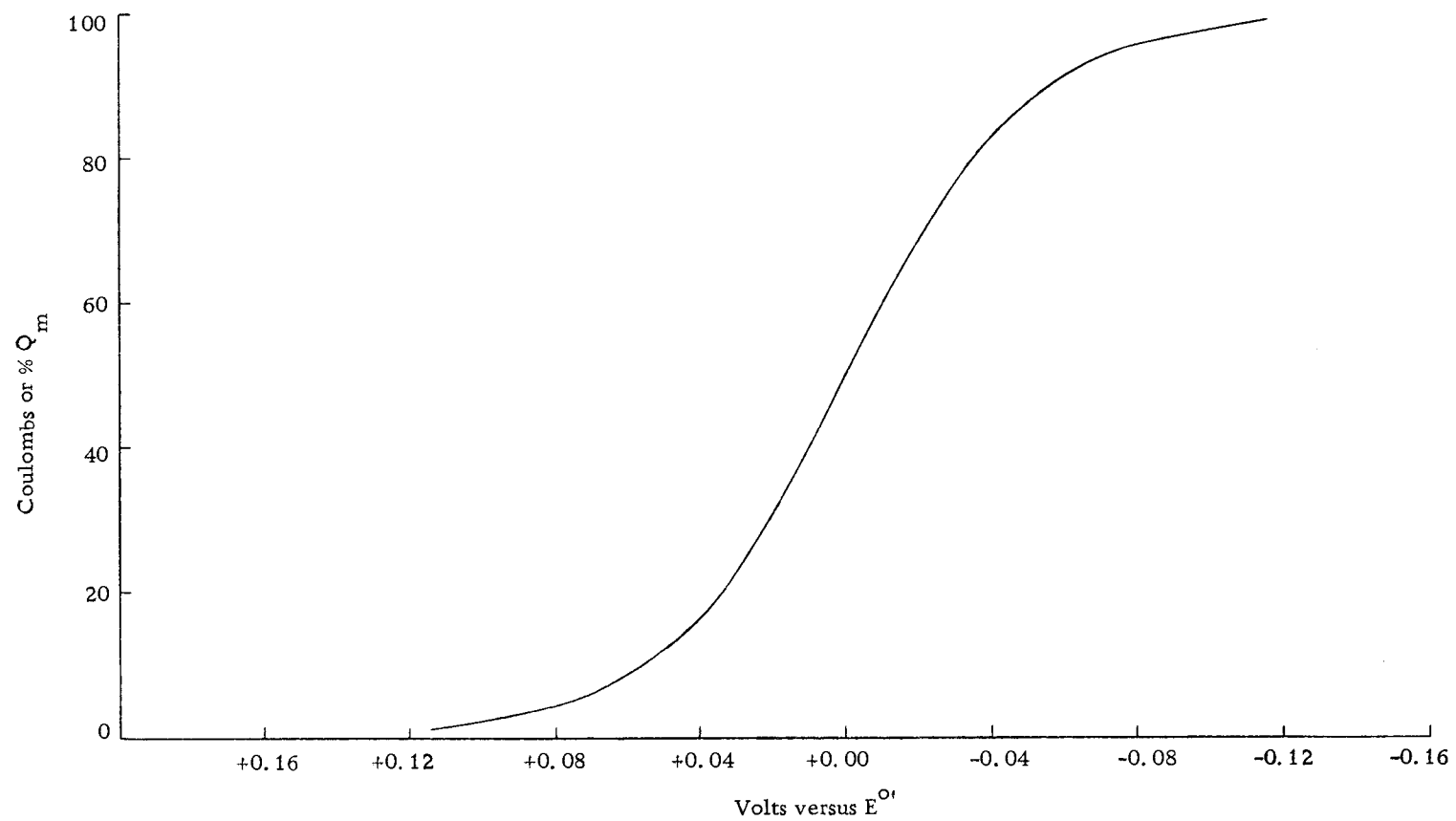


Figure 1. A plot of the Nernst equation.

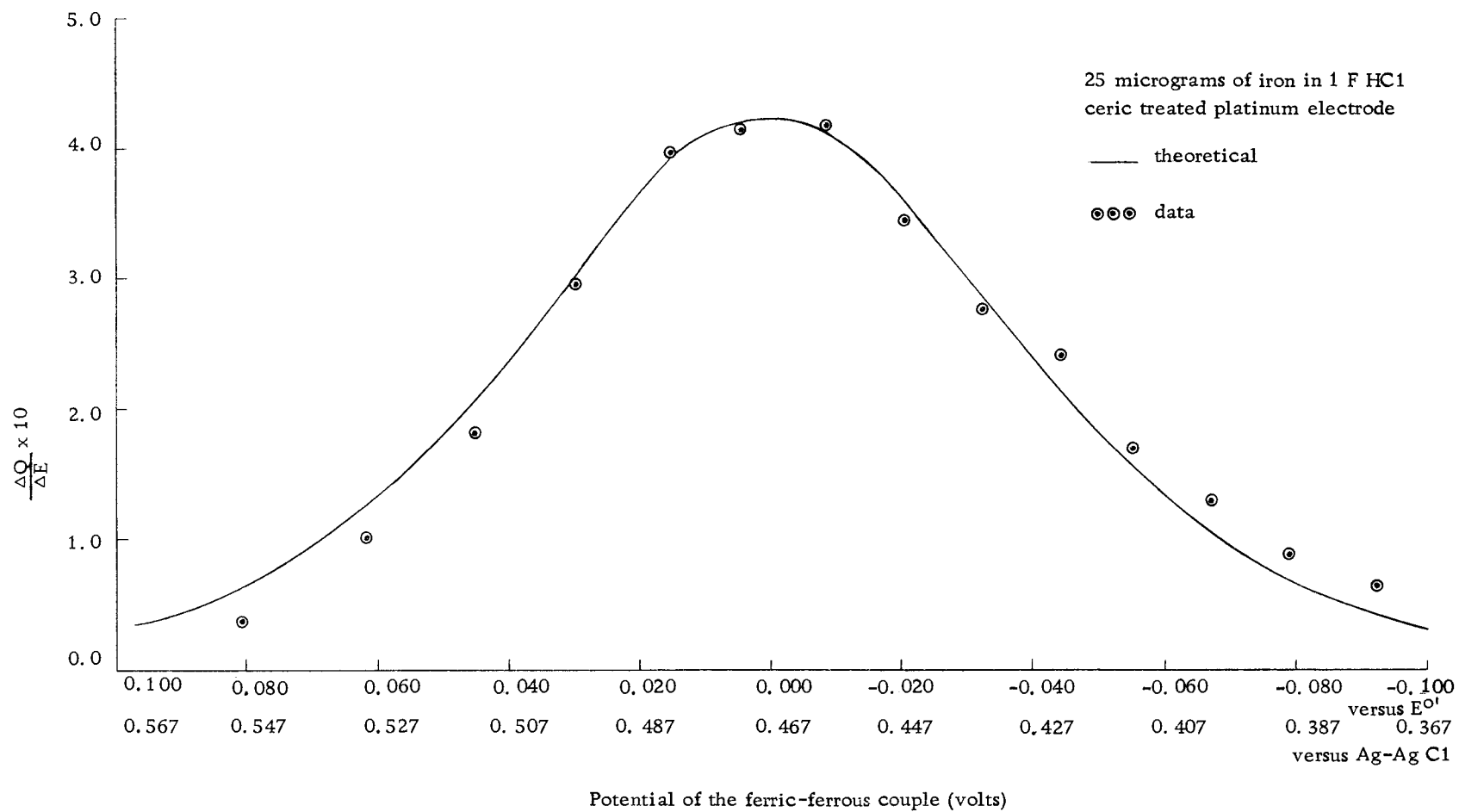


Figure 2. Theoretical and experimental $\Delta Q/\Delta E$ plot.

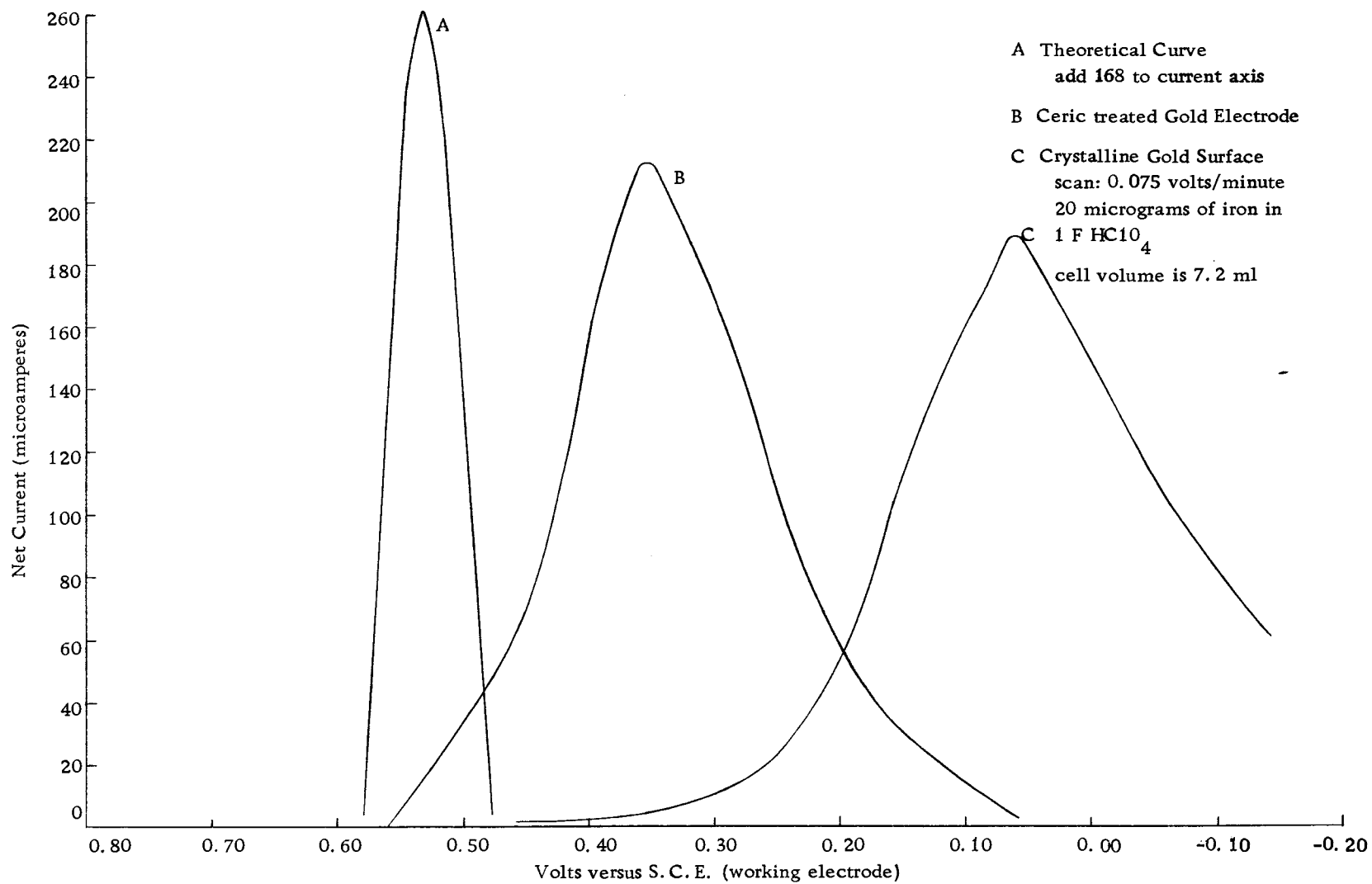


Figure 3. Experimental and theoretical current-voltage plots for iron.

setting it equal to zero, the location of the maximum value of dQ/dE is found:

$$-\frac{d^2Q}{dE^2} = \frac{nF}{RT} \left(\frac{dQ}{dE} \right) \left(1 - \frac{2Q}{Q_m} \right) = 0. \quad (9)$$

Equation 9 shows that the maximum of dQ/dE occurs when $Q = \frac{1}{2}Q_m$.

Substituting this into Equation 6 yields

$$\left(\frac{dQ}{dE} \right)_{\max} = \frac{-nFQ_m}{4RT} \quad (10)$$

or

$$\left(\frac{dQ}{dE} \right)_{\max} = \frac{-n^2 F^2 Q_m}{4RT}. \quad (11)$$

Simplifying Equation 11 yields the expression obtained by Scott (28)

$$(i)_{\max} = \frac{-n^2 F^2 Q_m}{4RT} \text{ (voltage scan rate)}. \quad (12)$$

As mentioned previously, this derivation applies only when both the oxidized and reduced species are present as ions in solution.

The development of dQ/dE now needs to be considered for an electrochemical system in which the reduced species is a metal.

The major difference between the development of equations for metal deposition and the above electrochemical system results from the activity of the reduced metal.

Kolthoff and Lingane (14, p. 203-4) assume the activity of a metal deposit to be unity for polarography; although, they do mention that when trace amounts of metal deposition are involved, the activity may differ from unity. Work by Rogers and co-workers (8, 10, 25, 26) and Peekema (22, p. 57) indicate that for the deposition of trace amounts of silver, the activity of the deposit is much smaller than unity. Rogers (25) developed several forms of the Nernst equation for the deposition of different amounts of metal. The derivation of dQ/dE for metal deposition that is presented here was treated in more detail by Peekema (22, p. 10).

The activity of a metal deposited on the surface of an inert electrode can be considered unity only when the electrode is covered completely with the metal being deposited. This implies that the electrode is behaving as if it were made of the metal being deposited. The Nernst equation for a metal deposit with an activity of one has the form of

$$E = E_m^{\circ} + \frac{RT}{nF} \ln A_{\text{ox}}. \quad (13)$$

The symbol E_m° represents the standard potential of the metal's half-reaction compared to the normal hydrogen electrode. Treating Equation 13 in a manner similar to Equation 1 yields

$$\frac{-dQ}{dE} = \frac{nF}{RT} (Q_m - Q). \quad (14)$$

The maximum of dQ/dE is represented by

$$\left(\frac{dQ}{dE}\right)_{\max} = \frac{-nFQ_m}{RT}. \quad (15)$$

For deposition on an inert electrode involving less than a one monolayer deposit, Rogers (25) and Peekema (22, p. 13) considered the activity of the monolayer to be represented by Equation 16

$$A_{\text{red}} = f_{\text{red}} \cdot \frac{z}{z_o}. \quad (16)$$

The symbol f_{red} has its usual significance, while z is the amount of a metal deposited and z_o is the amount of a metal required to form a monolayer of a metal deposit. Substituting Equation 16 into Equation 1 yields

$$E = E^{o'} + \frac{RT}{nF} \ln \frac{x}{z}, \quad (17)$$

where

$$E^{o'} = E^o + \frac{RT}{nF} \ln \frac{f_{\text{ox}} z_o}{f_{\text{red}} v}.$$

The symbol v represents the volume of the solution. Equation 17 is algebraically identical to Equation 2, so the equations derived for the electrochemical system with both the oxidized and reduced species present as ions in solution will apply here, also.

Peekema (22, p. 13) developed an empirical equation to describe the activity of metal deposits intermediate between the above two limiting cases. This equation has the form of $A_{\text{red}} = 1 - \exp(-z/z_o)$. It can be substituted into Equation 1, and an equation similar to Equation 6 can be derived (22, p. 14).

Peekema (22, p. 15) also derived an equation for the mercuric-mercurous and iodine-iodide couples. He obtained

$$\frac{dQ}{dE} = \frac{-nF}{RT} \left[\frac{Q(Q_m - 2Q)}{Q_m + 2Q} \right] \quad (18)$$

and

$$\left(\frac{dQ}{dE}\right)_{\text{max}} = \frac{nFQ_m}{RT} \left[3/2 - \sqrt{2} \right]. \quad (19)$$

A convenient parameter for comparing theoretical and experimental current-voltage plots is the peak width at one-half of the peak height. This will be referred to as half-width and be symbolized by $w_{1/2}$. A detailed treatment of the derivations leading to $w_{1/2}$ can be obtained from work by Peekema (22, p. 17).

For electrochemical systems with both the oxidized and reduced species present as ions in solution and also metal deposition of less than a monolayer, Peekema (22, p. 17) shows that from Equation 6

$$w_{1/2} = \frac{0.0906}{n} \text{ volts.} \quad (20)$$

The symbol n represents the number of electrons per atom involved

in the reduction or oxidation. For gross deposits of metal, it is shown that from Equation 13,

$$w_{\frac{1}{2}} = \frac{0.0178}{n} \text{ volts.} \quad (21)$$

III. EXPERIMENTAL

Cell Design

The two cells used in this work are shown in Figures 4 and 5. The cell in Figure 4 is identical to the one used by Peekema (22, p. 22), which has a platinum gauze working electrode. The cell used for much of the work in this study differs in that it has a gold gauze working electrode. It is shown in Figure 5.

The side arms on each of the cells are used to separate the auxiliary and reference electrodes from the working electrode compartment. One side arm contains the auxiliary electrode and its supporting electrolyte. The auxiliary electrode consists of a platinum wire dipped in one molar perchloric acid. The other side arm contains the reference electrode and its salt bridge (one molar ammonium nitrate). The reference electrode is a silver wire in a solution saturated with potassium chloride and silver chloride contained in a Pyrex glass tube. The reference electrode solution is connected to the salt bridge solution by a crack in the glass tube formed by placing a soft glass bead on the end of the glass tube containing the reference electrode.

The glass frits separating the cell compartments are plugged with silica gel to minimize the transfer of solution between

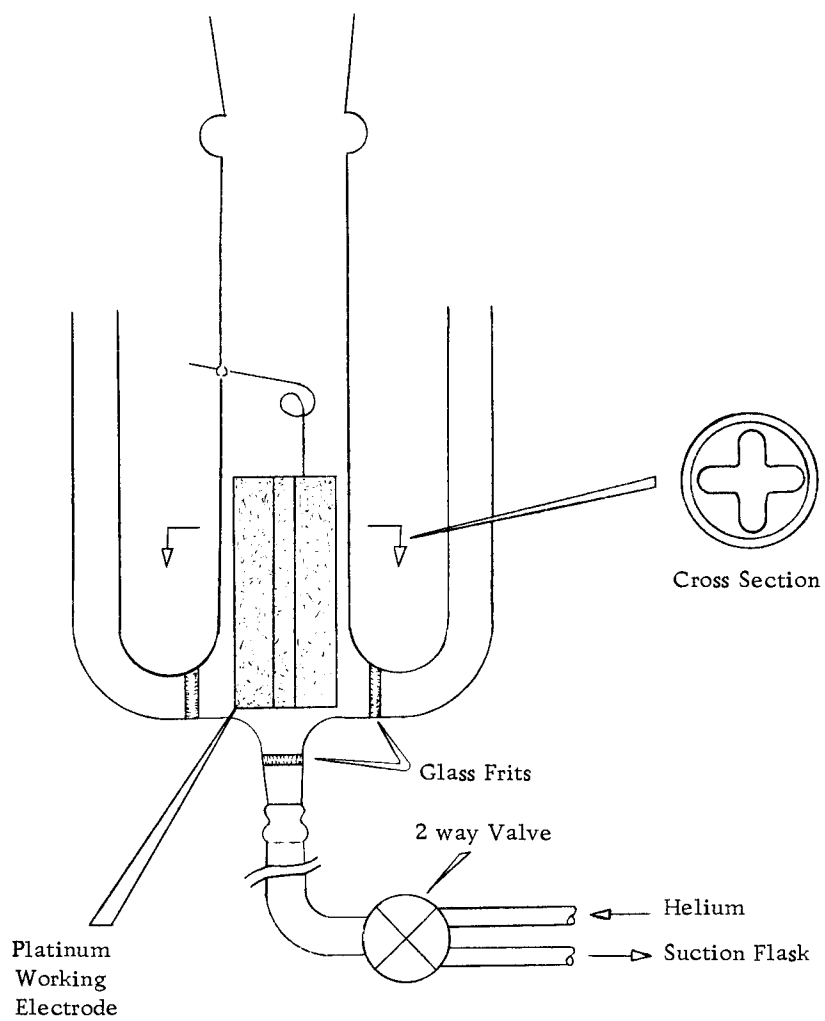


Figure 4. Cell I.

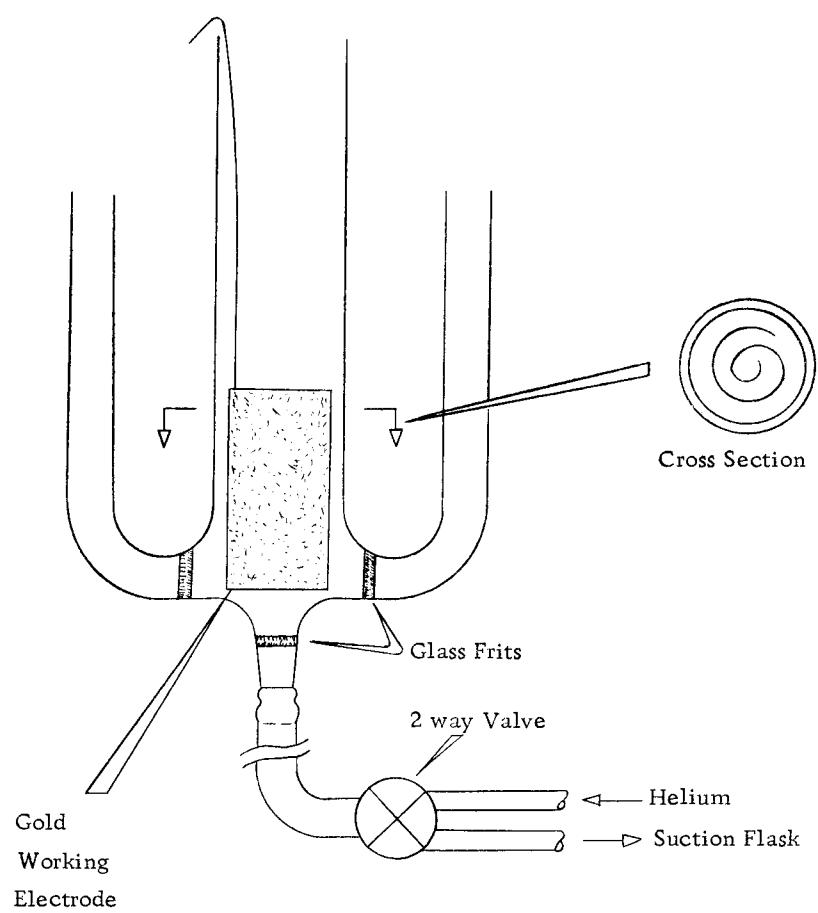


Figure 5. Cell II.

compartments. A concentrated solution of sodium silicate is placed on the surface of the dried frits. A vacuum is applied to the working electrode compartment to draw some of the silicate solution into the frits. One molar perchloric acid is then added to the side arms and working electrode compartments to precipitate silicic acid within the pores of the frits.


To determine if the frits are properly plugged, distilled water is placed in all three compartments with a higher water level in the side arms. If any measurable change in the liquid levels becomes observable after a 12 hour period, the frit must be plugged again as just described.

The cell is drained by turning the two-way valve (Figure 4 or 5) so that the cell solution is drawn into a suction flask connected to a vacuum line. When the drain frit becomes plugged, it may be cleaned by drawing some distilled water through it, turning on the helium sparge to force the solution back through the frit into the cell, and then withdrawing the solution from the top of the cell. This is the only cleaning that the cell normally requires.

To prevent diffusion of oxygen into the cell while an electrolysis is in progress, the top of the cell is plugged with paper tissue (Kimwipe). Since the gas sparge causes considerable spray, it is necessary to have sufficient walls above the solution so that the liquid spray will run down the walls and back into the solution without

wetting the tissue paper in the top of the cell. The amount of solution lost during an electrolysis was found to be insignificant.

Instrumentation

The instrument used in this work is similar to one described by Enke and Baxter (4). A block diagram of the instrument is shown in Figure 6. The symbol, , represents a chopper stabilized operational amplifier.

This instrument's basic function is that of a potentiostat. It maintains the potential between the working and reference electrodes at any desired value by passing current between the auxiliary and working electrodes. It must be realized that the potentiostat will function only as long as its operational amplifiers are not current or voltage limited.

The operational amplifier (1) functions as an integrator, providing a linear ramp voltage which can be either positive or negative. This provides the scan voltage. Amplifier (2) is used to sum the voltage signals from the sweep generator, initial potential section and amplifier (3). Amplifier (3) is a Deford Voltage Follower (19, p. 363). It allows a voltage signal to be drawn from the reference electrode without drawing significant current (less than 10^{-10} amperes) through it. Amplifier (4) serves to maintain the potential of the working electrode at a virtual ground and to convert the

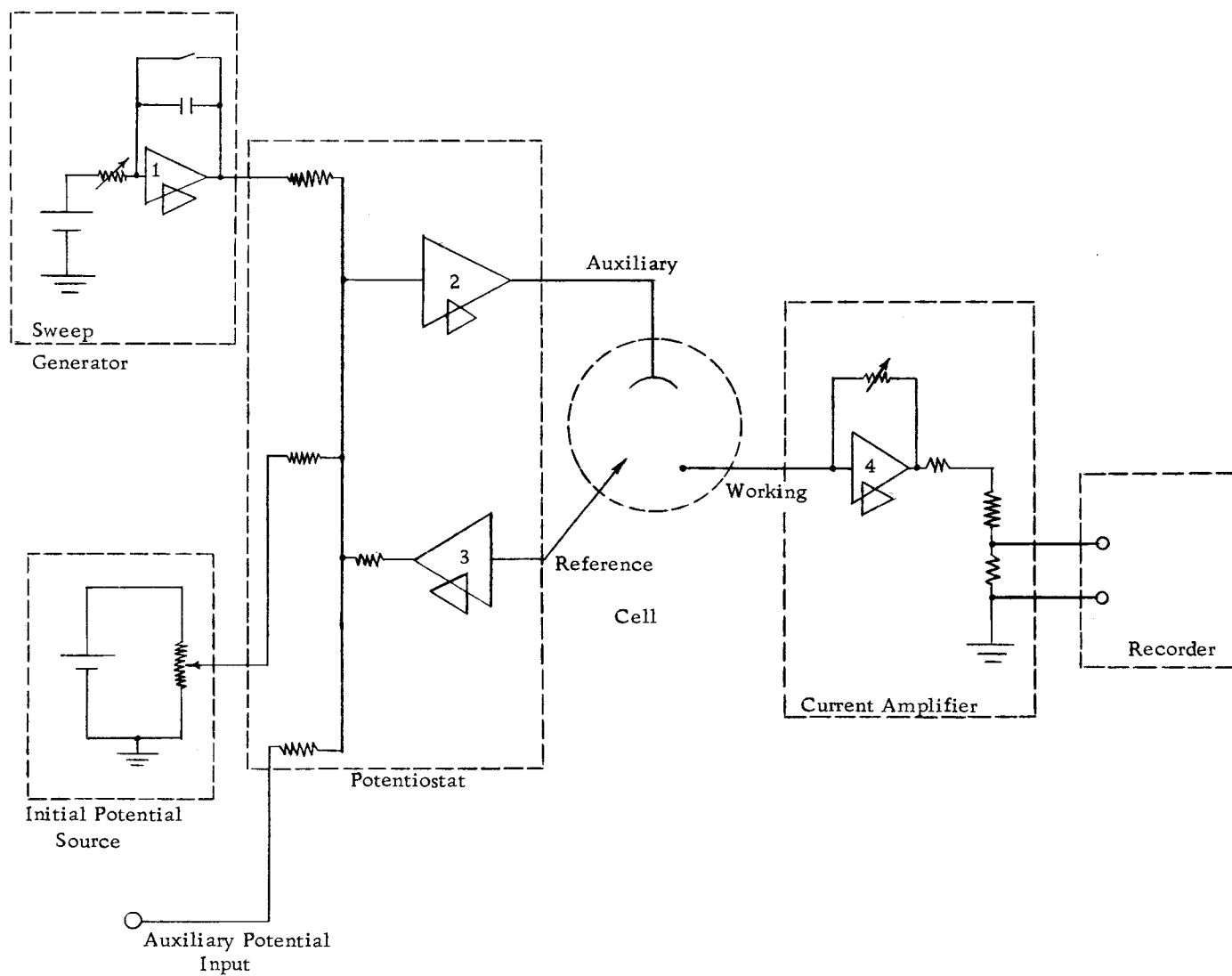


Figure 6. Block diagram of the voltage scanning coulometer.

current flowing through it into a voltage signal of suitable magnitude for measuring. The potentiostat functions as a result of amplifier (2), summing up all of its inputs. If they do not sum up to zero, a large current will flow through the auxiliary-working electrode loop until the potential measured between the reference and working electrodes is equal and of opposite sign to the three voltage inputs (sweep generator, initial potential source and auxiliary potential input).

The recorder used with this instrument must be capable of measuring both positive and negative potentials during any given experiment. A normal experiment consists of a reduction voltage scan followed by an oxidation voltage scan. The currents flowing during each scan have opposite signs.

One other instrumental arrangement was used in this work. To study the ferric-ferrous couple it became necessary to add a fourth indicating electrode to the cell to correct for polarization of the working electrode. The potential of the indicating electrode was measured by connecting the indicating electrode to the glass electrode input of a Heath Recording Electrometer (Model EUW-301), and connecting the reference electrode input to the circuit ground.

The chemicals used in this work were all reagent grade and were diluted to desired concentrations with distilled water. The standard iron solution was prepared by dissolving iron wire in

hydrochloric acid. Iron in a chloride free solution, for work with the gold electrode, was prepared by fuming iron dissolved in hydrochloric acid in one molar perchloric acid until hydrogen chloride fumes quit coming off the solution. A 0.05 molar silver nitrate solution was prepared by dissolving silver nitrate crystals in distilled water. This solution was analyzed for silver ions by precipitating them as silver chloride and weighing the precipitate. A standard solution of potassium iodide was prepared by dissolving potassium iodide crystals in distilled water. For deaeration and stirring, helium gas was used without further purification.

Procedure

1. The supporting electrolyte is added to the cell with a 10 milliliter graduated pipet. Usually, 7 milliliters was added.
2. The solution is deaerated with helium gas at the rate of about 200 cc per minute for about five minutes.
3. The potentiostat is turned on and the working electrode is controlled at some initial potential, usually 0.8 or 0.9 volts versus the silver-silver chloride reference electrode.
4. The sample is next pipetted into the cell with either a 0 to 0.1 milliliter or 0 to 1 milliliter pipet. The sample volume was usually less than 1 milliliter.

5. After waiting a few minutes for the sample to be deaerated, the experiment is started. A normal experiment begins with an initial potential of 0.80 volts applied between the working and reference electrodes. The potential between the working and reference electrodes is scanned from the initial potential to 0.0 volts. The direction of the voltage scan is then reversed, and a scan from 0.0 to 0.80 volts is made, concluding the experiment.
6. The potentiostat is turned off and the cell drained at the end of the experiment. The cell must be rinsed thoroughly with distilled water before the above procedure may be repeated.

IV. RESULTS AND INTERPRETATION OF DATA

Ferric-Ferrous Couple

The ferric-ferrous couple was used to check the equations derived in the theoretical section and to illustrate the effects of electrode treatments on electrode reactions.

Data presented in Figure 3 illustrate some of the difficulties encountered in the comparison of experimental and theoretical curves. In Figure 3, three different curves are shown. Curve A is the theoretical current-voltage plot calculated from Equation 8 for the reduction of 17 micrograms of ferric ion. Curve B illustrates the experimental current-voltage plot for the reduction of ferric ion at a ceric treated gold surface, and Curve C results from the reduction of ferric ion at a crystalline gold surface. It is evident that the electrode treatment has a profound effect on the reduction of ferric ions, as illustrated by Curves B and C in Figure 3. An explanation for the effect of the electrode surface on this reaction appears in the following section on electrode treatments.

The difference between the theoretical curve and the experimental data in Figure 3 is attributed to polarization¹ of the working

¹ Polarization is considered here to be the difference between the potential of the ferric-ferrous couple and the potential applied between the working and reference electrodes.

electrode. This conclusion was reached also by Peekema (22, p. 35) for similar work. The greatest polarization illustrated by Curve C shows the effect of the electrode surface on the kinetics of an electrode reaction.

The reconciliation of the experimental data and theoretical curve shown in Figure 3 requires that the potential of the working electrode be corrected for polarization. This was accomplished by adding a fourth electrode to the cell. The potential of the ferric-ferrous couple was then measured with respect to circuit ground, using the apparatus described in the experimental section of this thesis. The data obtained with this apparatus is plotted in Figure 7 and shows the indicating electrode potential versus the potential of the working electrode. Figure 8 is obtained from Figure 7 by subtracting the potential of the indicating electrode from the applied potential of the working electrode. This is (in effect) the measurement of the indicating electrode potential against the reference electrode instead of against ground as was done in Figure 7. Figure 8 is a plot of the ferric-ferrous couple's potential versus the applied potential of the working electrode.

Figure 9 is a plot of current versus the potential of the indicating electrode. This plot was made using the data contained in Figures 8 and 10 and indicates that the potential of the ferric-ferrous couple changes less than 200 millivolts during the entire reduction scan.

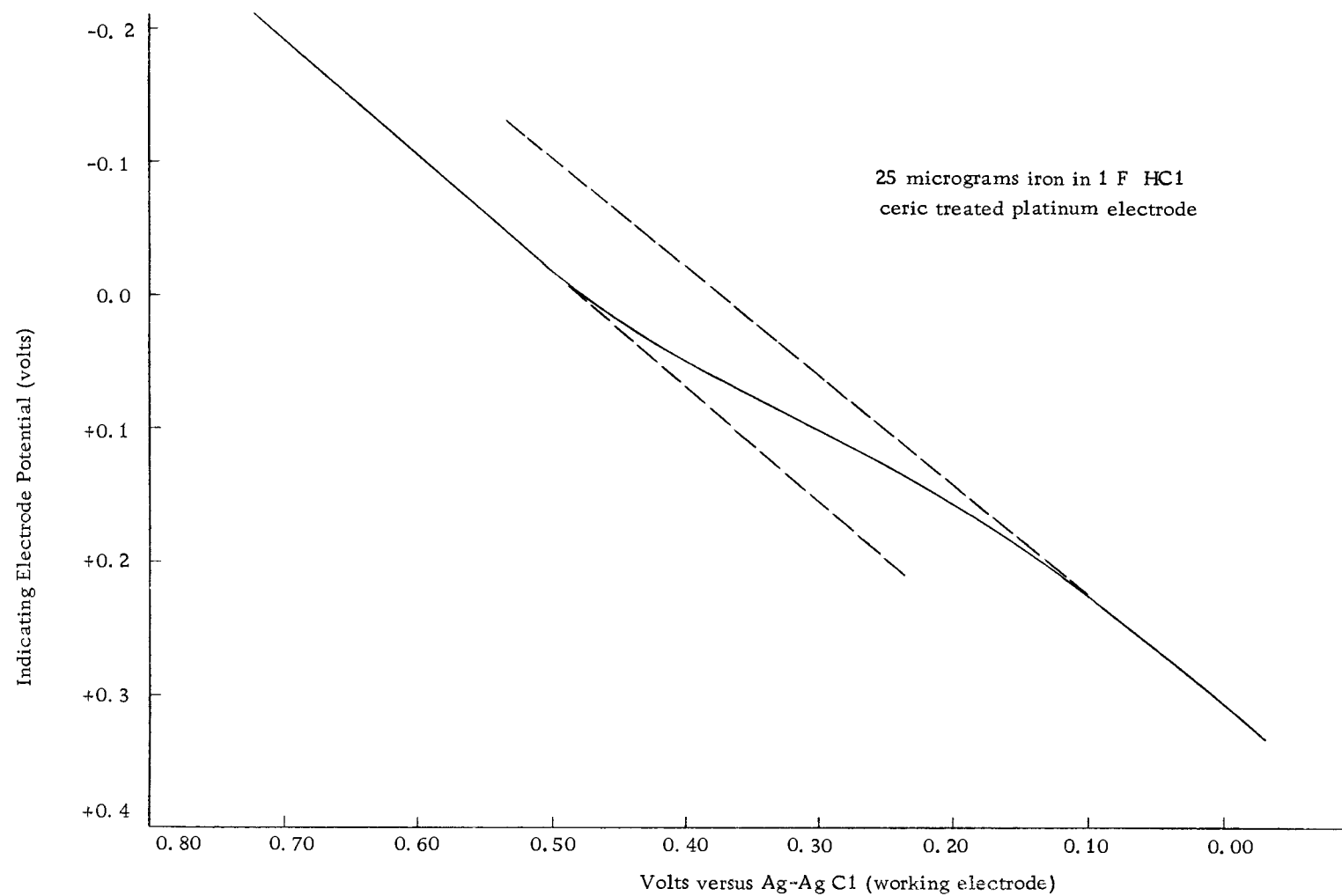


Figure 7. A plot of indicator electrode potential versus working electrode potential I.

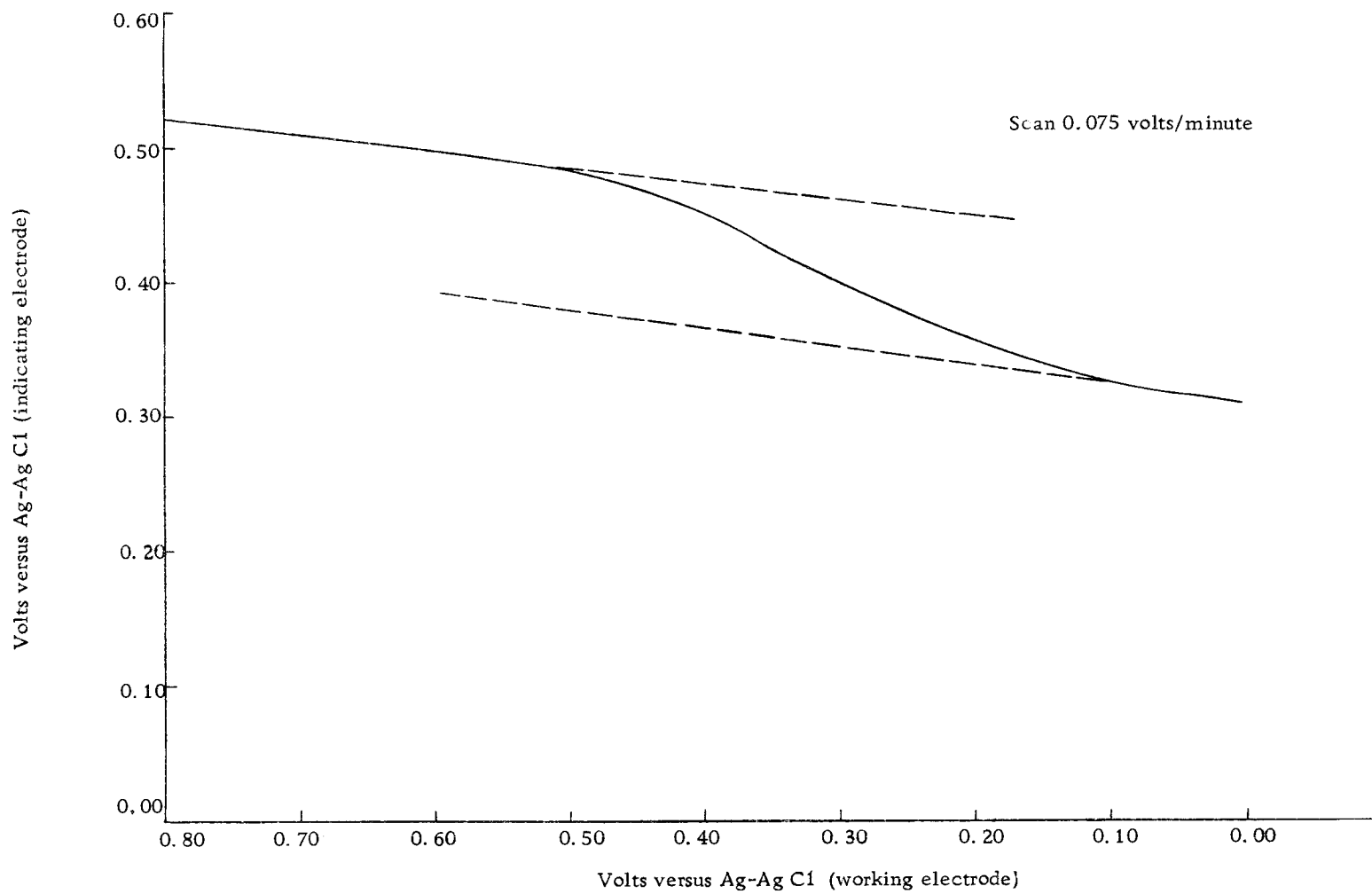


Figure 8. A plot of indicator electrode potential versus working electrode potential II.

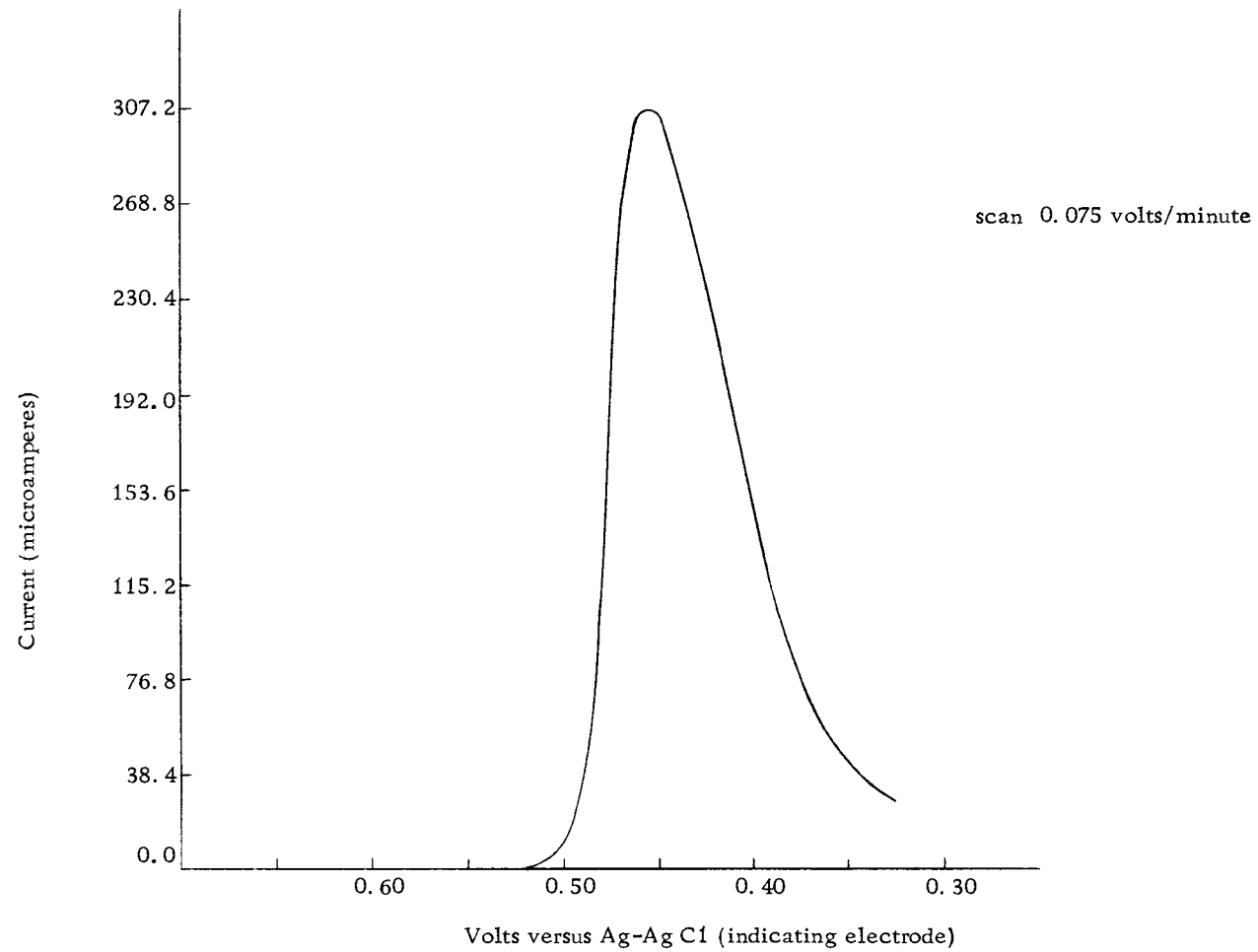


Figure 9. Current versus potential of indicating electrode.

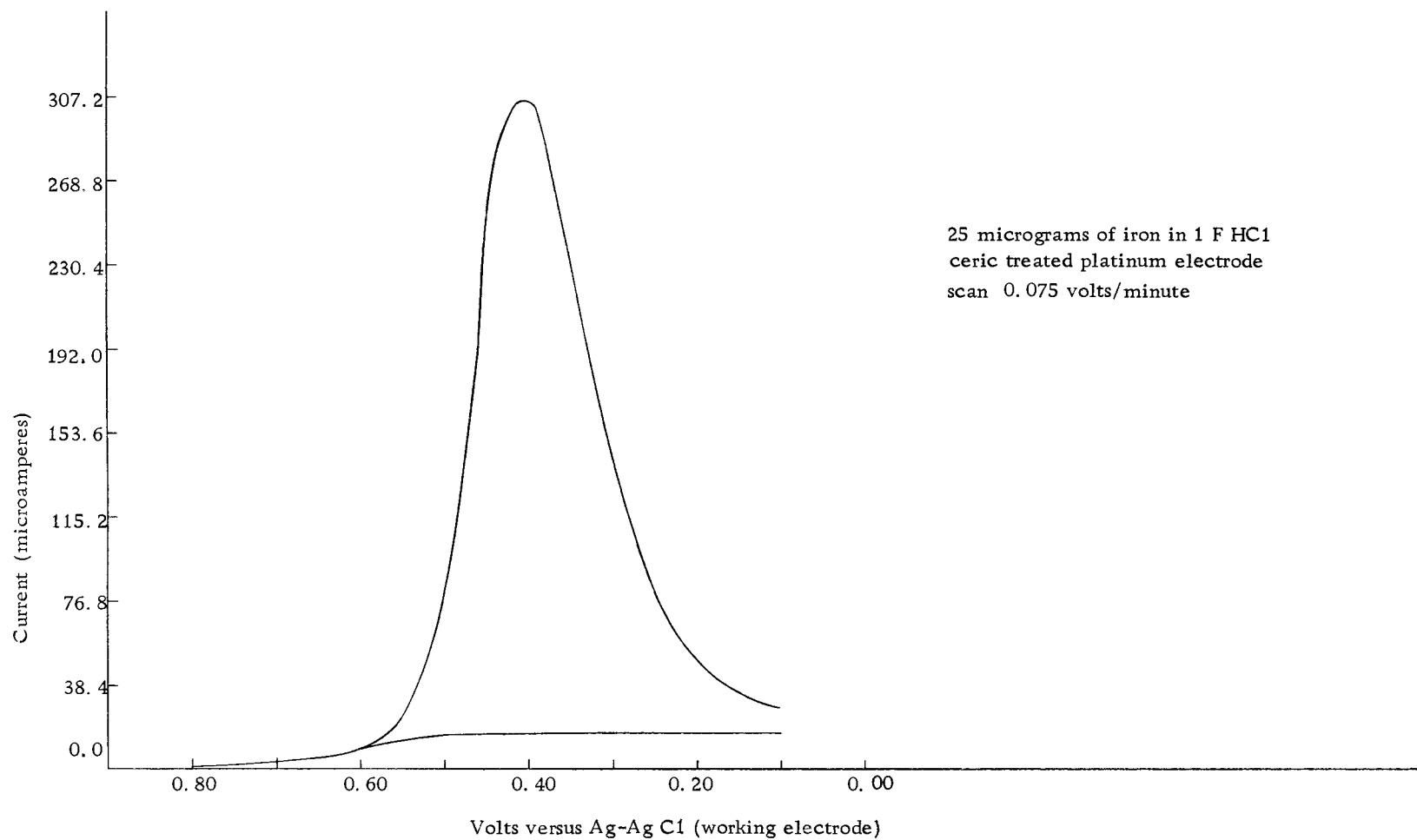


Figure 10. Experimental current-voltage plot for iron.

This is reasonable, for when the working electrode is controlled at 0.80 volts, the small current that flows is principally due to oxidizing the surface of the electrode and to oxidizing the solvent. These electrolysis products should, in no way, effect the potential measured by the indicating electrode. At the end of a voltage scan, when the working electrode is controlled at 0.0 volts, the reduction of the solvent accounts for most of the current flowing through the cell. The reduction of the solvent has little effect on the potential measured by the indicating electrode.

The potential measured by the indicating electrode versus silver-silver chloride is primarily that of the ferric-ferrous couple. When the ratio of the concentrations of ferric and ferrous ions is either very large or very small, the indicating electrode does not register the true couple potential. At these concentration ratios of ferric and ferrous ions, the potential measured by the indicating electrode is susceptible to the potentials of other electroactive species.

The above discussion explains the data in Figure 8. Figure 8 shows that the working electrode is controlled at 0.80 volts, while the indicating electrode measures only 0.52 volts. As the potential of the working electrode is scanned negatively, a potential is reached where most of the current flowing is the consequence of ferric ion reduction and, at this point, the indicating electrode potential begins

to follow the working electrode potential as shown in Figure 8. When the end of the reduction scan is approached, the indicating electrode measures 0.3 volts, while the working electrode is at 0.0 volts.

The theoretical dQ/dE versus E plot was calculated from Equation 7, and this is illustrated, along with the plot of the experimental data in Figure 2. The current-voltage plot obtained experimentally is included in Figure 10. The conversion of the experimental current-voltage plot to the theoretical dQ/dE versus E plot was accomplished as follows:

1. The area under the current-time plot was calculated for a given time interval and this value is ΔQ .
2. The change in the potential of the ferric-ferrous couple (indicating electrode) over the above time interval yields ΔE .

The above data yields $\Delta Q/\Delta E$, which is plotted in Figure 2. To compare the theoretical and experimental plots, $E^{O'}$ is assumed to be the potential of the ferric-ferrous couple at the current maximum on the current-voltage plot. Figure 2 shows good agreement between experimental and theoretical curves, indicating that the ferric-ferrous couple is reversible. The $\Delta Q/\Delta E$ plot suffers from the limitation that it is incremental rather than a continuous derivation; but, as is illustrated, this is not a serious limitation.

Figure 11 was obtained by plotting current against $\Delta E/\Delta T$, where E is the potential of the indicating electrode and T is time.

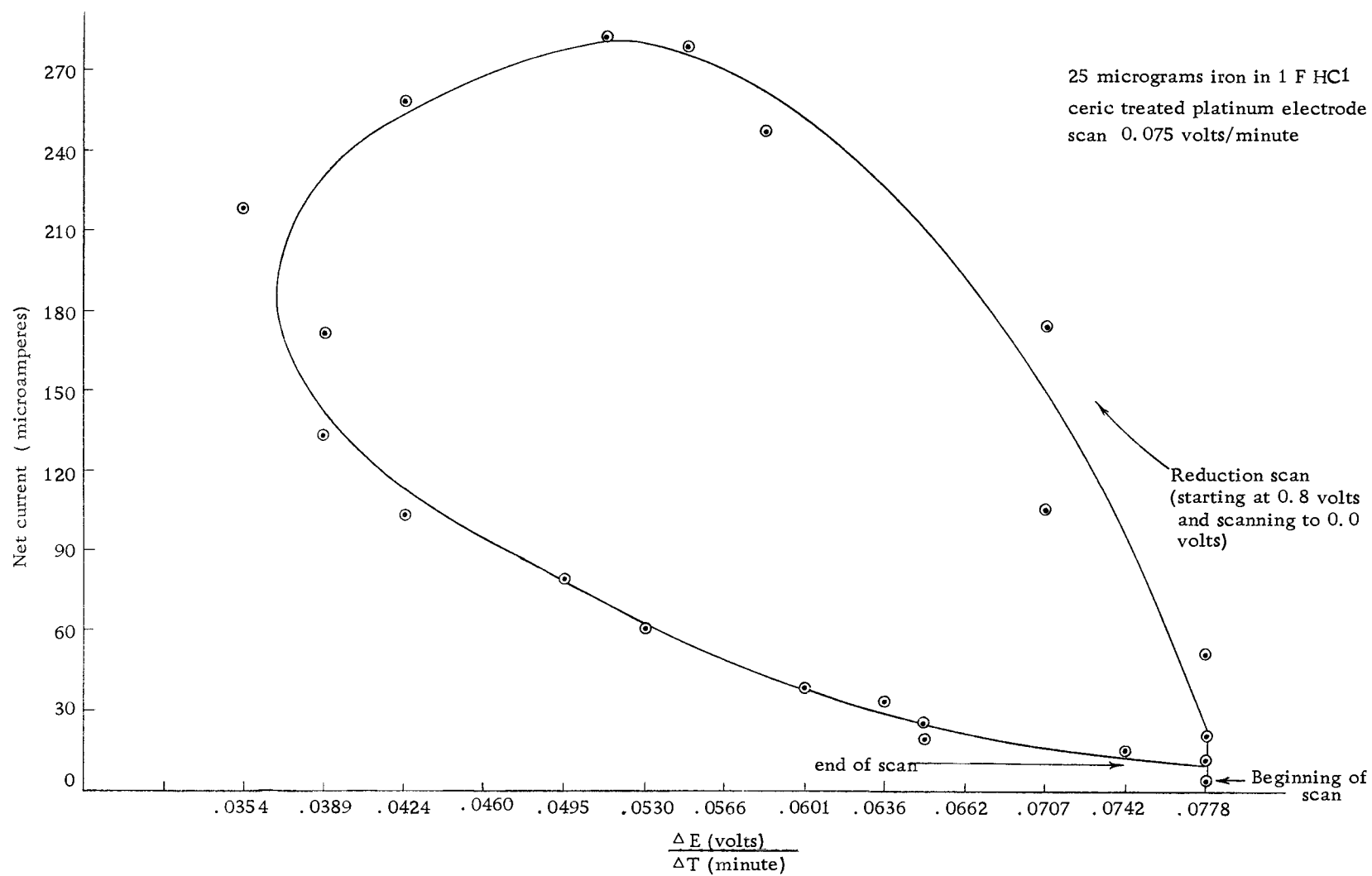


Figure 11. Hysteresis curve.

This is, in effect, a hysteresis loop, resulting from the polarization of the working electrode during a reduction scan of ferric ions. As the current through the cell increases, the rate of change of the indicating electrode potential decreases. This seems to indicate that the potential is controlled by the kinetics of the ferric ion reduction even though the potential of the working electrode is changing at a constant rate. It is also observed from Figure 11 that the $\Delta E/\Delta T$ at the beginning and end of the reduction scan is the same as the applied voltage scan rate.

The amount of polarization of the working electrode at the current peak can be determined using the fourth indicating electrode (as above) or by the following method. The amount of polarization can be found by taking one-half of the difference in the applied potential of the working electrode at the current peak for the anodic and cathodic scans. This method is applicable only when both the oxidized and reduced species are ions in solution. It assumes that the amount of polarization is the same for the oxidation and reduction scans.

The data in Table 1 were calculated using the latter method from different oxidation and reduction scans for iron at 25° C.

Peekema (22, p. 48) found, using a platinum working electrode, the same trends in polarization with the electrode surface condition as shown in Table 1. Looking again at Table 1, it is noted that as successive runs are made, the polarization of the electrode

increases. More on the relationship of the above data to the electrode reaction appears in the following section on electrode treatments.

Table 1. Polarization of the working electrode.

Polarization (millivolts)	Electrode	Electrolyte	Electrode Treatment
56	platinum	1 F HCl	Ceric
56	platinum	1 F HCl	Ceric
103	gold	1 F HClO ₄	*Ceric (first scan after treatment)
124	gold	1 F HClO ₄	*Ceric (second scan " ")
149	gold	1 F HClO ₄	*Ceric (third scan " ")
749	gold	1 F HClO ₄	KI-H ₂ SO ₄
> 749	gold	1 F HClO ₄	KI-H ₂ SO ₄

*Cell drained, rinsed, and new solution added between each experiment.

Electrode Treatments

After observing the effects of the electrode treatments on the iron current-voltage plot, it seems important to investigate the treatments that make rough and crystalline surfaces and to determine the effects of these surfaces on the mechanism of the ferric ion reduction.

To prepare a gold or platinum electrode with a crystalline surface, the following procedure is used. The electrode is placed

in one molar perchloric or sulfuric acid and the potential of the electrode is maintained at 1.25 volts versus silver-silver chloride until the current through the cell drops to about 10 microamperes. The cell is then drained and a solution of 0.05 molar sulfuric acid and 0.1 molar potassium iodide is added. The electrode is soaked in this solution for about five minutes (22, p. 52).

Anodizing the electrode covers its surface with an oxide film. Anson (3) has found chemical evidence of platinum oxides on the surface of platinum electrodes after being anodized or treated with a ceric solution. Laitinen (16) has used coulometry to measure the extent of surface oxidation on platinum and gold electrodes.

When the electrode is anodized (moderately), only the most active metal atoms will be oxidized. The most active metal atoms are considered to be those atoms not in the regular metal lattice. The metal oxide is dissolved by the potassium iodide-sulfuric acid solution (22, p. 54), resulting in a clean, crystalline surface, with most of the metal atoms in their normal lattice positions.

Some problems were encountered in attempting to remove all of the iodine from the cell and this was particularly a problem in the work with silver. Even with extensive washing, the presence of iodine remained in the cell.

Peekema (22, p. 54) attributed the presence of iodine to an adsorbed layer on the electrode surface. Anson (12, 21) has recently

published work substantiating the adsorption of iodine on a platinum surface. The iodine can also be adsorbed on the surface of the silica gel, plugging the frits of the cell. Several techniques were found by this writer to minimize this source of iodine contamination:

1. Prepare the potassium iodide-sulfuric acid solution immediately prior to use so that the iodine concentration is at a minimum.
2. Soak the cell overnight in distilled water.
3. Make a reduction scan to reduce the iodine, shut off the potentiostat and drain the cell.

The open circuit cell potential for the ceric treated gold electrode was measured before and after the potassium iodide-sulfuric acid solution was added to the cell. These measurements yielded 0.92 volts versus silver-silver chloride before the sulfuric acid solution was added and 0.28 volts after it was added. The cell was filled with one molar perchloric acid for each of these measurements. The crystalline electrode surface obtained from the above treatment is ideal for studying the deposition of metals; but, as was already shown, it is very undesirable when studying a system like the ferric-ferrous couple.

The ceric treatment of the platinum or gold surface consists of soaking the electrode in 0.2 N ceric solution for approximately five minutes. The solution is then drained and the electrode is placed in one molar perchloric acid and reduced at 0.0 volts versus

silver-silver chloride until the current through the cell drops to approximately 15 microamperes.

Several reduction scans for the ceric treated gold and platinum electrodes are included in Figures 12 and 13. They illustrate the effect of the treatment for providing a low blank current and provide experimental evidence for the formation of metal oxides on the surface of the electrodes. The reduction scan of the ceric treated platinum electrode and of the anodized platinum electrode, as in the crystalline electrode treatment, results in similar current-voltage plots. The current maximum occurs at the same potential in each case indicating that each treatment forms the same metal oxide.

The reduction of a metal oxide on the surface of the electrode results in an electrode whose surface is coated with finely divided particles of metal (1). For a platinum electrode, this process is referred to as platinizing the surface. This electrode treatment would be expected to roughen the surface of an electrode. As mentioned previously, this activated metal surface catalyzes the ferric-ferrous reduction and oxidation.

Anson (2) postulated that the mechanism of the ferric-ferrous couple involves, at least in part, adsorption on the surface of the electrode. The ceric electrode treatment could conceivably cause two changes in its surface. It could increase the surface area of the electrode or form activated sites on its surface. Anson (1)

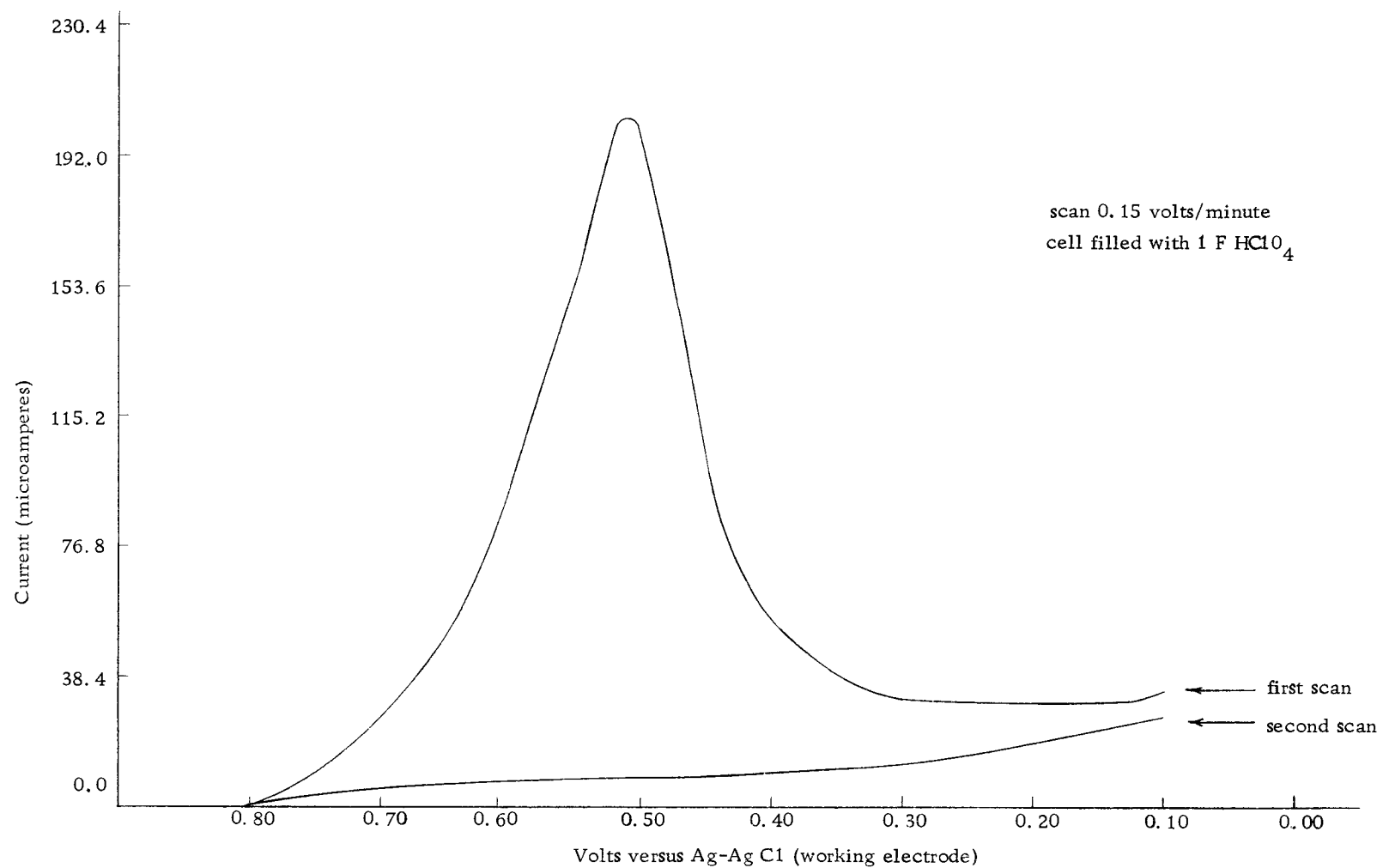


Figure 12. Reduction scans of the ceric treated platinum electrode.

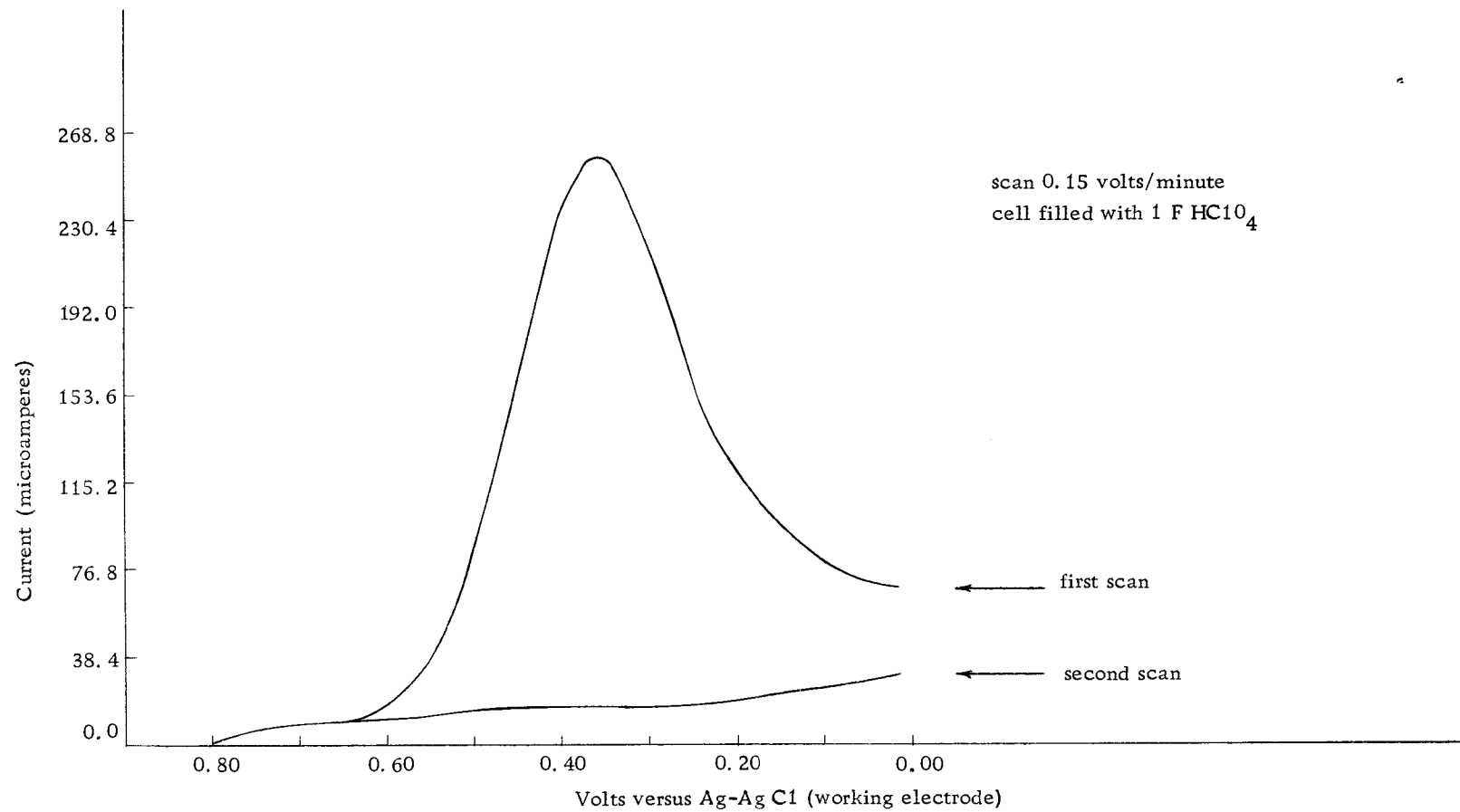


Figure 13. Reduction scans of the ceric treated gold electrode.

postulates that light platinization of an electrode does not change its surface area appreciably. So, it appears that the effect of the ceric treated electrode on the ferric-ferrous couple is due largely to the activated sites catalyzing the reaction.

A possible mechanism (27) for the transfer of an electron by the ferric-ferrous couple is considered in the following. If we assume that the electrode is covered by two layers of solvent molecules, then a ferric ion could exchange one of its waters of hydration for one in the outer layer on the surface of the electrode. The electron is then passed through the potential barrier of the electrode-solution interphase (double layer) to the ferric ion (27). After the reduction, the ferrous ion could either diffuse away from the electrode to make room for the incoming ferric ion or bond through a water of hydration to another ferric ion. The electron could then be transferred from the electrode to the ferric ion through the ferrous ion.

Since the largest energy barrier for this reaction is across the solution-electrode interface, it seems likely that if a surface metal atom is in an activated state, it could pass electrons at a higher energy level through the energy barrier easier than a metal atom of lower energy, thus catalyzing the ferric-ferrous couple.

Referring to the data in Table 1, it is observed that as successive voltage scans are run, the polarization of the working electrode increases. Anson (1) reported that the active surface sites

can age (become less active) and that the electrode must be oxidized and reduced to again obtain the active sites. It seems reasonable to assume that as a scan is made, a certain amount of electropolishing (migration of atoms on the surface) of the electrode can take place, thus removing the active sites and forming a more crystalline electrode surface. To obtain maximum sensitivity in the determination of iron, Scott (28) gave the electrode an oxidation and reduction treatment during each analysis. This also supports the above hypothesis.

Silver Deposition

The previous section on electrode treatments illustrated the effects of the electrode surface on the electrochemistry of the ferric-ferrous couple. The section presented here illustrates the effects of the electrode surface on the deposition and stripping of silver.

Rogers and co-workers (8, 10, 25, 26) studied the deposition of microgram amounts of radioactive silver on various metal electrodes with controlled potential coulometry. Their work showed the effects of electrode surfaces and metals on the potential where trace amounts of silver will deposit. Peekema (22, p. 56) studied the deposition and stripping of microgram quantities of silver at a smooth platinum electrode with voltage scanning coulometry.

The current-voltage plots obtained from the deposition of trace

amounts of silver on a crystalline gold electrode surface are shown in Figure 14. Before discussing these data in detail, the following conventions regarding current peaks will be adopted. The peaks that occur at potentials anodic to 0.35 volts will be referred to as monolayer peaks. The one large peak that appears around 0.25 volts will be called the reversible peak. This arbitrary convention will be explained later in this section.

The concentration of silver in the cell for the current-time plots shown in Figure 14 is approximately 10^{-5} molar. From Latimer (17, p. 197), the potential of the silver ion-silver metal couple is listed as 0.799 volts versus the normal hydrogen electrode or 0.600 volts versus the silver-silver chloride reference electrode used in this work. Assuming the activity of the silver deposit to be unity, it can be calculated from Equation 13 that no silver deposition should occur until about 0.30 volts (is reached in the deposition scan), versus silver-silver chloride. According to this form of the Nernst equation, silver should dissolve off of the electrode in a 10^{-5} molar silver nitrate solution at potentials greater than 0.30 volts versus silver-silver chloride.

From Figure 14, it can be seen that a large amount of silver deposition occurs at potentials positive to 0.30 volts. In order for this to occur the activity of the silver deposit on the gold electrode must be much less than unity. The activity of the silver deposit

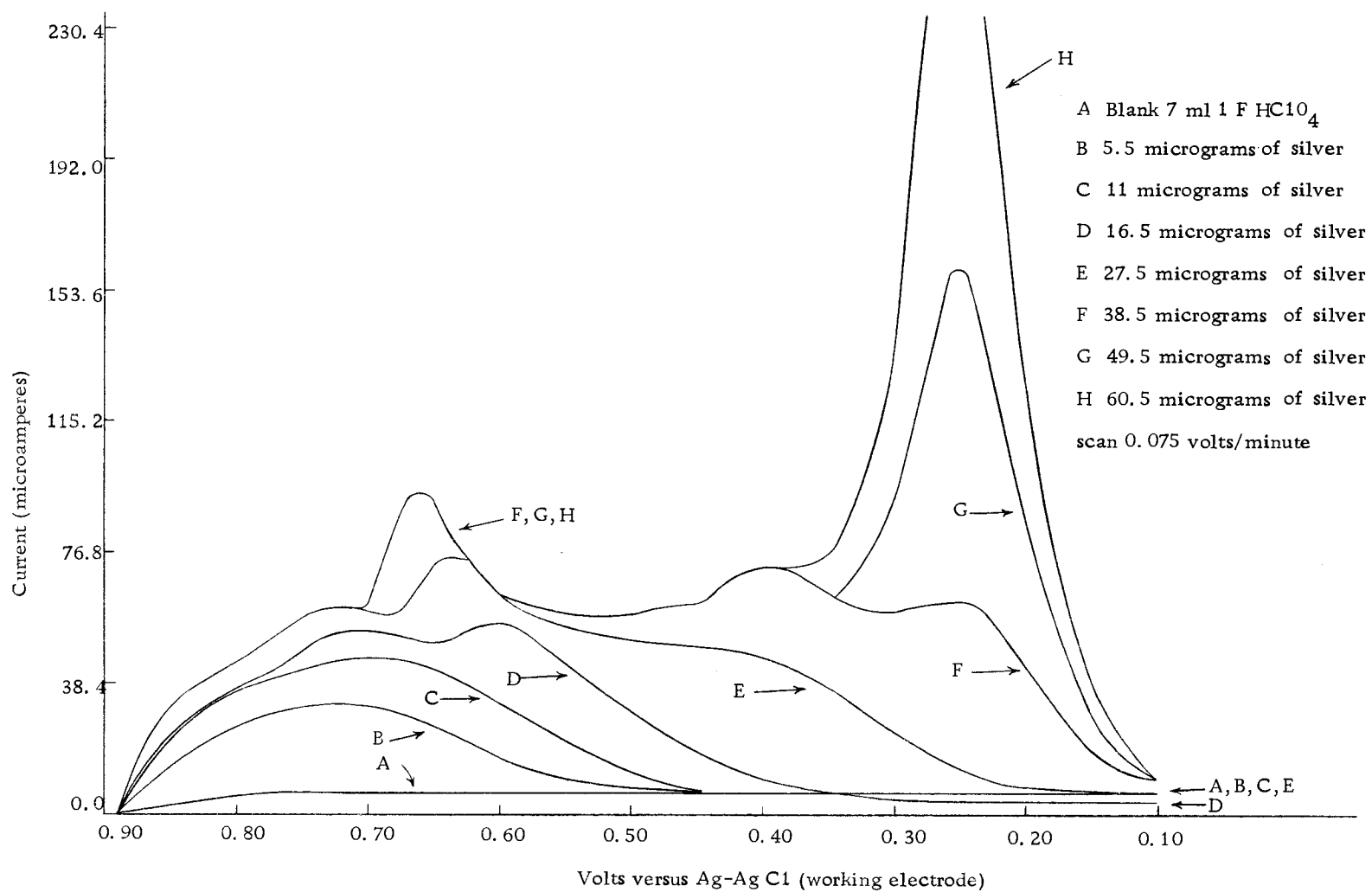


Figure 14. Silver deposition on the crystalline gold surface.

would be expected to be smaller than unity if gold and silver have an affinity for one another. Rogers (24, p. 39) states that gold and silver form a solid solution with one another with placement of silver atoms in the gold lattice. Conway's (9) calculations show that a lattice site has a much lower potential energy than a position at random on the surface of a metal. As a result of their tendency to form an alloy with one another, the silver atoms prefer to plate on the gold surface before depositing on silver atoms. Because silver can be deposited in stable sites on the surface of the gold electrode, it is often difficult to remove all of the silver from the electrode.

When one of the chemical electrode treatments (discussed in the previous section) is not used to clean the working electrode, the following procedure may be used. With the potentiostat controlling the potential of the working electrode at either 0.80 or 0.90 volts, the solution is drained from the cell until just enough is left to maintain electrical contact between the electrodes. Fresh one molar perchloric acid is added to the cell and, after the current decays to a few microamperes, the solution is again drained as above. This procedure is continued until very little current flows through the cell upon addition of fresh perchloric acid.

Referring again to Figure 14, it is seen that as small amounts of silver nitrate are added, (5.5 or 11 micrograms) a single broad peak occurs at 0.7 volts versus silver-silver chloride. Depositing

more silver (27.5 micrograms), causes a second peak to appear at about 0.63 volts. With still more silver (38.5 micrograms), deposited on the electrode, a third peak appears at about 0.40 volts. The reversible peak appears at 0.25 volts when more silver nitrate is added to the cell and subsequently deposited.

It can be seen from Figure 14 that there are several peaks in the monolayer region of the current-voltage plot. These peaks indicate that the surface of the electrode must be somewhat crystalline so that the adsorption energies would be clustered around several discrete values. Conway and Bockris (9) calculated adsorption energies for silver deposition at three lattice sites: a planar surface, an edge, and a kink. Since there are three peaks in the monolayer region of the plot, these could result from deposition at the above three lattice sites. If the electrode surface is amorphous, then we would expect a continuous display of adsorption energies with no particular value appearing more often than another.

Each change in the activity of the silver deposit by a factor of ten shifts the potential where deposition can occur by 0.059 volts according to Equation 1. Since most of the silver monolayer is deposited by at least 0.45 volts during the deposition scan, a value of 0.01 sets the upper limit for the activity of the silver monolayer deposit.

Since the amount of silver deposited in the monolayer region

of the current-time plot can be determined from Figure 14, the effective surface area of the electrode can be compared to its geometrical surface area. To do this we assume that the monolayer region corresponds to one layer of silver atoms. It seems reasonable to expect that the first monolayer of silver atoms will insulate the second layer of silver atoms from the attractive forces of the gold (22, p. 65). This will be discussed more thoroughly later in this section.

The following method was used to calculate the geometric surface area of the gold gauze electrode. Since the gold electrode is just gold plated platinum gauze, knowing the weight of the platinum gauze and the density of platinum metal allows the calculation of the total volume that would be occupied by the electrode if it were a solid mass. Measuring the diameter of the wire strand in the gauze allows the calculation of the total length of wire in the electrode. From the length, the surface area of the wire, neglecting the ends, can be calculated. Knowing the weight of the gold plate and its density, the volume that this amount of gold would occupy if it were a solid mass of metal is calculated. Dividing the volume of the gold by the surface area of the platinum yields the thickness of the gold plate. The radius for the plated electrode is used to determine the surface area, as above. For the gold gauze electrode, the geometric surface area was calculated to be 39.4 square centimeters. From Curve G in

Figure 14, the amount of silver required to form a monolayer can be shown to be 2.27×10^{-7} moles when the silver that deposits with the addition of silver nitrate to the cell is included.

From Bockris (9), the radius of a silver atom is given as 1.44×10^{-8} centimeters. From this, it was calculated that 2.55×10^{-9} moles of silver are required to cover a square centimeter of electrode surface. From the experimental amount of silver required to form a monolayer, the effective to geometric surface area ratio for the crystalline electrode surface was calculated to be 2.3. From Curve B in Figure 19, the effective to geometric surface area ratio for the ceric treated gold surface was calculated to be 1.01.

Peekema's (22, p. 65) work on a crystalline platinum electrode yielded an effective to geometric surface area ratio of 2.6. Bowden and Rideal (7) compared the effective and geometric surface area of platinum and obtained a ratio of 2.1. The ratio obtained here for the crystalline gold surface is intermediate between the two above values.

Byrne and Rogers (8) obtained an effective to geometric surface area ratio of 1.08 and 0.98 for hammer-forged gold electrodes. Comparing the ratio obtained here for the ceric treated gold electrode and that of Rogers', indicates that their electrode had a surface similar to the one obtained here with the ceric treatment. Laitinen (16) obtained a roughness factor of 1.12 using a scaled down BET

measurement with krypton gas for platinum foil. This value was questioned by Peekema (22, p. 65).

With the potential of the working electrode controlled at 0.80 or 0.90 volts versus silver-silver chloride, some current flowed when silver nitrate was added to the cell. When a total of three milliliters of 5.1×10^{-4} molar silver nitrate was added, one milliliter at a time, a large current flowed through the cell with the addition of the first milliliter and a decreasing current flowed upon the addition of the second and third milliliters. This would seem to indicate that the silver deposited on the gold at this anodic potential is plated in certain very low energy sites. Since there can only be a limited number of these positions available, it is possible that most of these sites are filled from the addition of the first milliliter, leaving only a few low energy sites for the remaining silver atoms that are deposited. A plot of the amount of silver nitrate added to the cell versus the equivalents of silver that deposit on the surface of the crystalline gold electrode at a controlled potential of 0.90 volts showed points that fall close to a straight line. This indicates that as more silver is added to the cell, more of it will deposit at this anodic potential.

The deposition of silver on the ceric treated gold electrode was studied to illustrate the marked effect of the electrode surface on this reaction. Figure 15 includes several deposition current-voltage

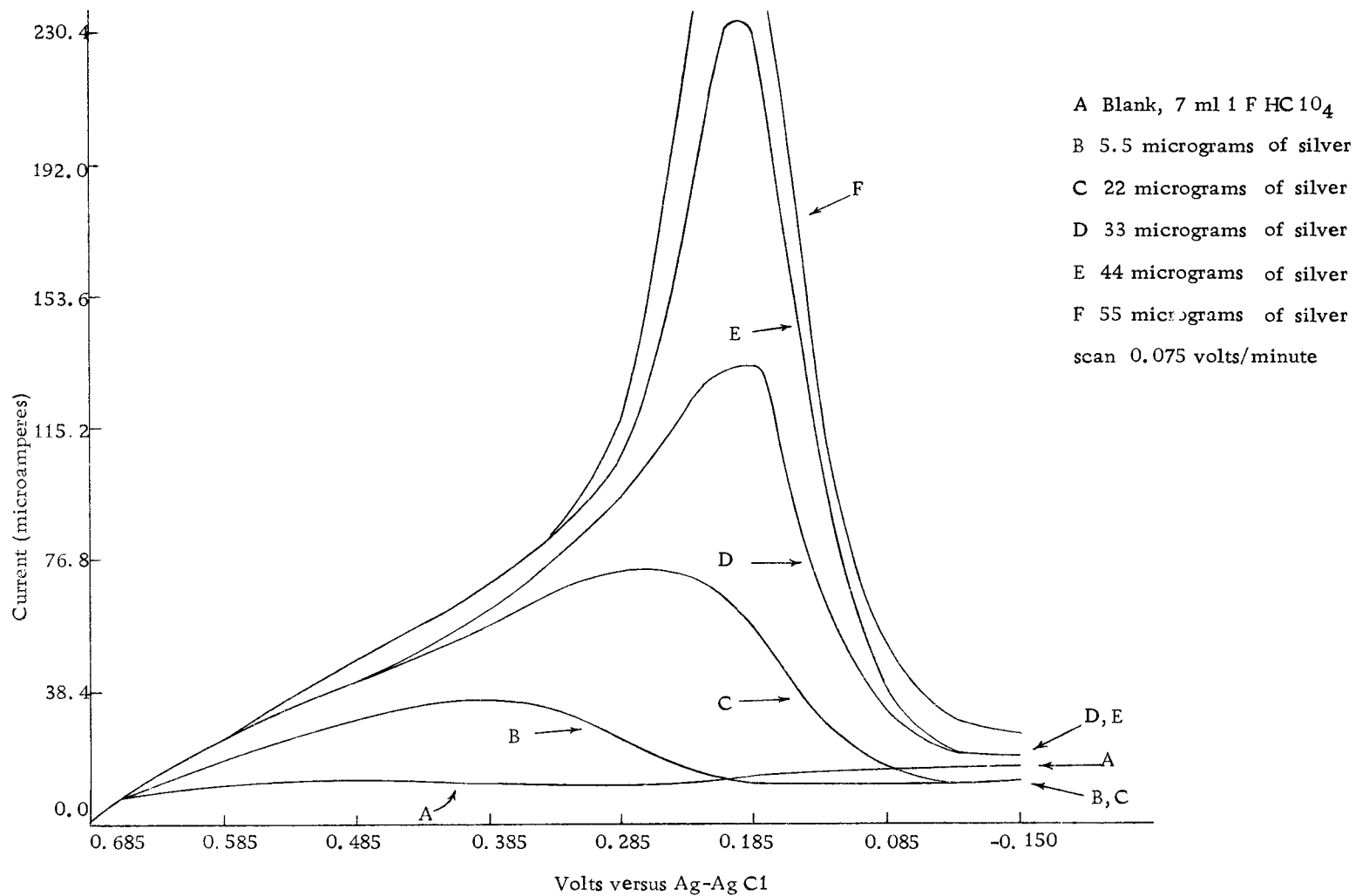


Figure 15. Deposition of silver on the ceric treated gold electrode.

plots for different amounts of silver deposited on the ceric treated electrode. There is a very obvious difference between the data in Figures 14 and 15. For a better comparison of silver deposition on crystalline and ceric treated electrode surfaces, Figure 16, is included.

From Figure 16, it can be seen that the activity of silver on the ceric treated gold electrode is much greater than for silver on the crystalline electrode surface. Also, it appears that the amount of silver deposited before the reversible peak appears is much less for the ceric treated electrode than for the crystalline electrode. Referring again to Figure 16, it can be seen that no peaks appear in the monolayer region of the current-voltage plot for the deposition of silver on the ceric treated electrode. It is concluded from this that the ceric treated surface is much less crystalline than the crystalline electrode surface. A possible explanation for the small amount of silver deposited in the monolayer region on the current-time plot results from the application of the mechanism for silver deposition developed by Conway (9).

Conway and Bockris (9) calculated the adsorption energy for silver deposition at three different sites--a planar surface, an edge, and a kink. Deposition at the planar surface has the lowest adsorption energy barrier (9). It would seem reasonable, then, that if a ceric treated electrode surface consists of very few planar

surface sites, then the size of the adsorption energy barrier would prevent deposition at large anodic potentials. As the voltage scan is made, a voltage would be reached ultimately where deposition could occur, in spite of the adsorption energy barrier. This occurs at 0.20 volts in Figure 16.

Comparing Figures 14 and 15, it can be seen that the potential for the current maximum of the reversible peak is closer to zero volts (at a higher energy level) for the ceric treated electrode surface than for the crystalline surface. This also seems reasonable due to the magnitude of the adsorption energy barrier at the rough electrode.

As was discussed previously, the reversible peak results from deposition on a surface whose activity is related to the fraction of the electrode surface covered by the silver deposit. For deposition on a crystalline platinum surface, Peekema (22, p. 62) considered the reversible peak to result from the second layer of silver atoms deposited on the electrode. Rogers (25) first related the activity of a metal deposit on an inert electrode to the fraction of the surface covered by the deposit. Relating the activity of a metal deposit to the fraction of an inert metal surface it covers is just an attempt to extend Raoult's Law to a monolayer deposit. This seems reasonable when the standard state of the deposit is considered to be the pure metal and the system being studied is reversible (22, p. 92).

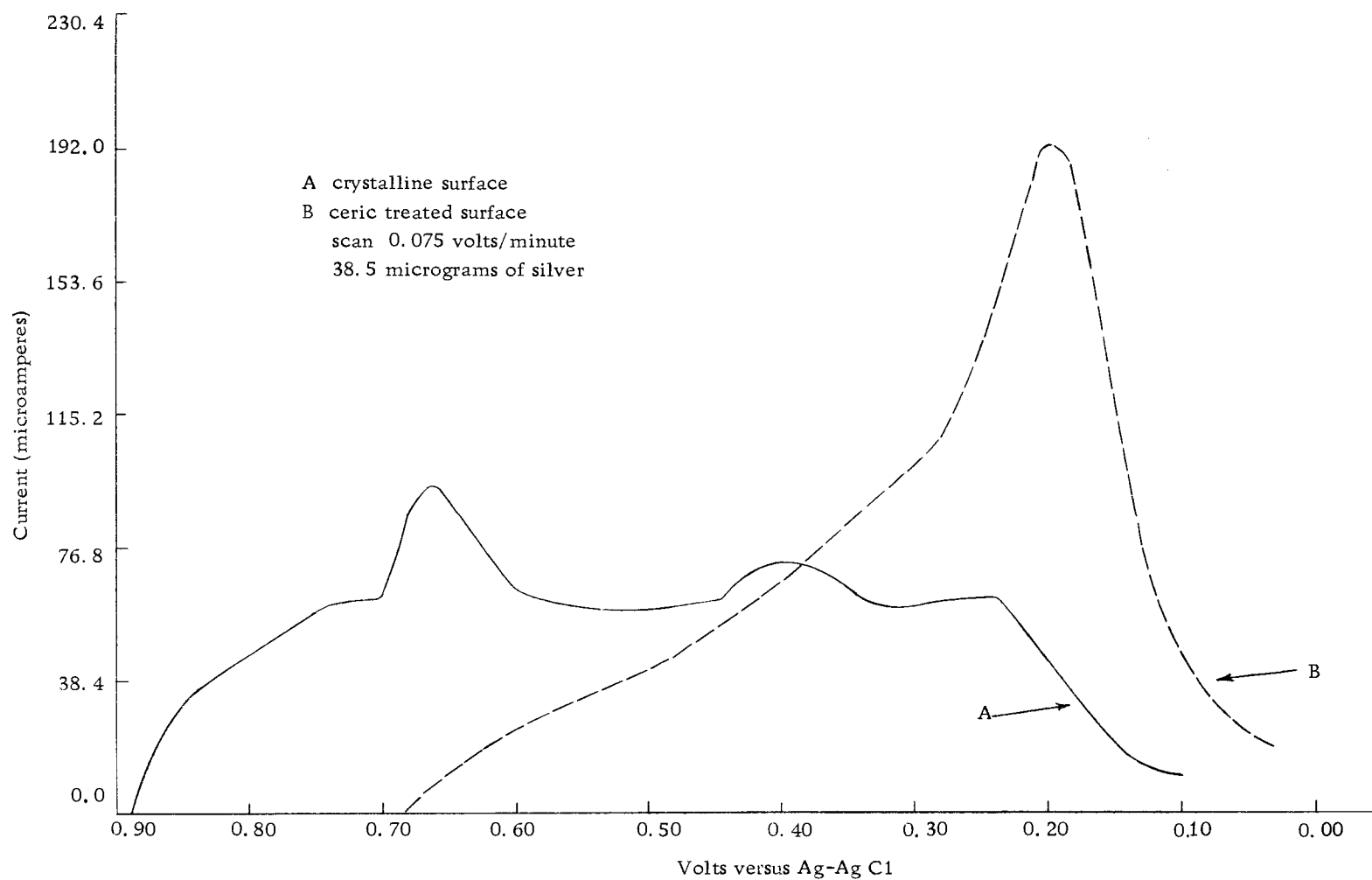


Figure 16. Deposition of silver on the gold electrode.

To obtain agreement between the theoretical and experimental stripping curves, Peekema (22, p. 63) ignored the effect of the first monolayer of deposited silver on the activity of the second layer. The theoretical and experimental stripping plots by Peekema (22, p. 63) agreed well when the activity of the second layer (reversible peak) was related to the fraction of the first layer covered by a second layer of silver atoms. This seems to be a reasonable assumption in light of the strong affinity between platinum and silver as represented by their phase diagram (30, p. 95). The first layer of silver atoms are acting as an insulation for successive layers so that the second layer may be deposited on an electrode that is truly inert and not on one that can form compounds or an alloy with the metal deposit.

As will be shown later, the stripping curve of silver from the ceric treated gold electrode follows the theoretical curve which assumes that the activity of the deposit is related to the fraction of the electrode surface covered with silver.

The area under the current-time plot in Figure 16 was determined for both the crystalline and ceric treated electrodes and agreement within three percent of one another was found. This is acceptable agreement within experimental error. This indicates that even though the initial potentials where the voltage scans were started, are different, substantial amounts of silver did not deposit on the electrode before the scan was started.

The deposition of silver on a ceric treated platinum surface was studied and it was found that it did not form any monolayer peaks, which is similar to the findings on the ceric treated gold electrode. The area under the monolayer current-time plot for the ceric treated platinum electrode was also much smaller as in the case of the ceric treated gold surface.

As shown by the current-time plot for the crystalline electrode in Figure 16, 38.5 micrograms of silver is not enough to form more than about one silver layer on the electrode. It would seem unreasonable that this same amount of silver could form more than one layer of silver on the ceric treated surface; in fact, it would be expected to cover less of the surface. The explanation used by Peekema (22, p. 62), that the reversible peak is the result of the deposition of a second or more silver layers seems unreasonable for the ceric treated gold surface.

After this lengthy discussion of silver deposition, it would be an oversight if we do not study the stripping of silver from various electrode surfaces. Figure 17 shows the stripping of various amounts of silver from the crystalline gold surface.

The stripping current-time plot is the exact reverse of the deposition plot. The first peak obtained upon stripping is the reversible peak and it is followed by the monolayer peaks. The area under the silver monolayer peaks upon stripping is the same as that upon

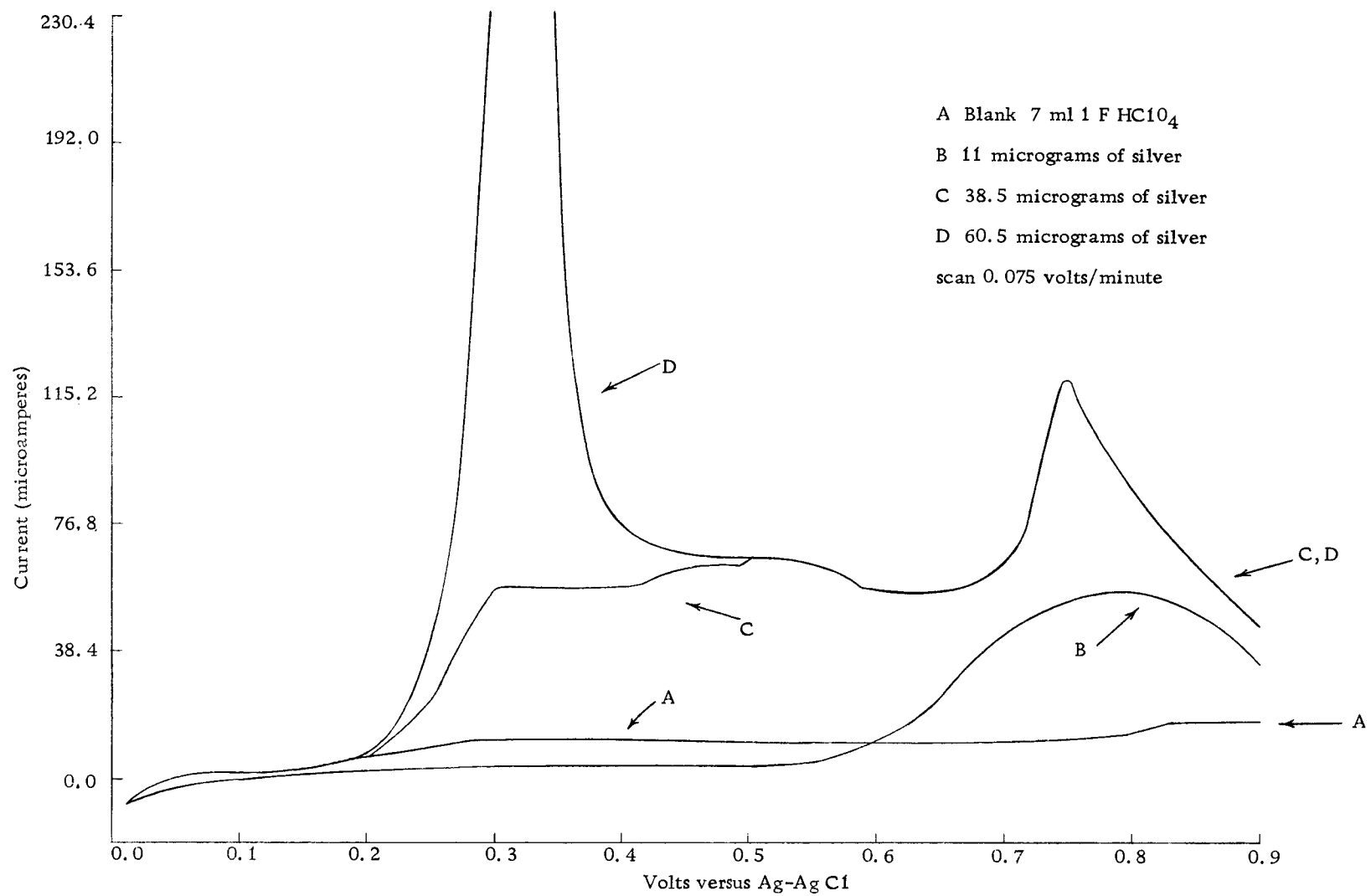


Figure 17. Stripping scans of silver from the crystalline gold surface.

deposition, within experimental error for Curve G in Figure 14. The areas under the reversible peaks for stripping and deposition also agree within experimental error.

The width of the reversible current peak at one-half of its height ($w_{\frac{1}{2}}$) for silver deposition is calculated to be 0.0906 volts (Equation 20). It should be remembered that this equation applies only for the deposition of silver when the activity of the deposit can be related to the fraction of the electrode surface covered. For gross deposits, it is recalled, from Equation 21, that the $w_{\frac{1}{2}}$ should be 0.0178 volts. If the amount of silver deposited is intermediate between gross and several monolayer amounts, the $w_{\frac{1}{2}}$ will also be between 0.0906 and 0.0178 volts.

The amount of polarization of the working electrode should be at a minimum during the stripping scan because all of the electro-active species needed for the oxidation are present on the electrode surface. Equations 7 and 20 should be applied only to the stripping scan since polarization is at a minimum. The polarization of the working electrode cannot be corrected here as was done in the iron case.

Figure 17 shows the stripping current-time plot for increasing amounts of silver at the crystalline gold surface. Stripping Curve D results in a $w_{\frac{1}{2}}$ of less than 0.0906 volts, indicating that the amount of silver deposited is intermediate between a several monolayer and

a gross deposit. The reversible peak appears at 0.325 volts with monolayer peaks at 0.52 and 0.75 volts.

Figure 18 illustrates a stripping scan with the proper amount of silver to yield a $w_{\frac{1}{2}}$ of 0.0906 volts. Also included in this figure is the theoretical stripping curve predicted by Equation 7. The exact amount of silver deposited previous to the potential, when the activity of the deposit becomes proportional to the fraction of the surface area covered, is not known accurately. This requires that the amount of silver deposited in forming the reversible peak be found by taking $(dQ/dE)_{\max}$ from the stripping curve and solving for m in Equation 11. As can be seen from Figure 18, there is good agreement between the theoretical and experimental curves, supporting the assumption that polarization of the working electrode can be neglected during a stripping scan.

The curves in Figure 18 also support the assumption that the activity of the deposit is proportional to the fraction of the electrode surface covered by the deposit. The experimental curve leaves the theoretical curve at 0.41 volts, where the silver monolayer peaks begin to appear.

Several qualitative observations can be made concerning the stripping scans shown in Figures 17 and 19 for crystalline and ceric treated electrodes. As was observed from the deposition scans on the ceric treated gold electrode (Figure 15), the apparent size of the monolayer upon stripping is much smaller on the ceric treated electrode surface than on the crystalline surface. In Figure 19, the reversible stripping peak appears at 0.385 volts for the ceric treated

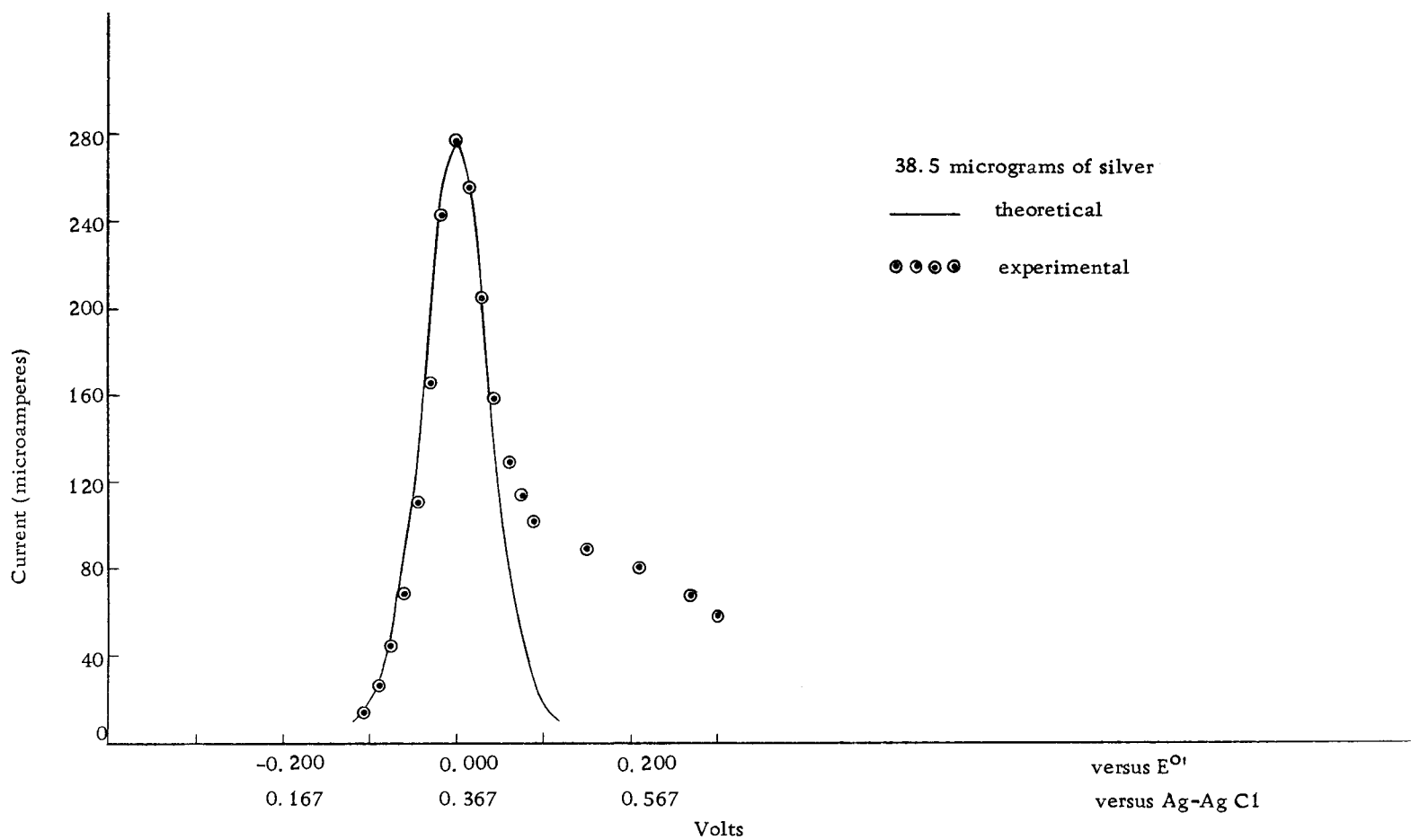


Figure 18. Theoretical and experimental silver stripping curves at the ceric treated gold surface.

electrode. Figure 17 shows the reversible stripping peak occurring at 0.325 volts for the crystalline electrode surface. This data agrees with Conway and Bockris (9), who showed that the potential energy of a metal atom in a kink or edge site is much lower than that for a metal atom deposited at a planar site. The desorption energy barrier is also greater for the transfer of an atom from an edge or kink site into the solution double layer. From the above discussion, it would be expected that a more anodic potential would be required to remove the silver atoms from the ceric treated electrode surface.

The discussion presented explaining the smaller size of the first monolayer deposited at the ceric treated electrode applies here, also. When the silver atom is stripped from the electrode surface, the same adsorption energy barrier that was present on the deposition scan is present on the stripping scan. The desorption energy, the affinity between the silver and gold metals, and the removing of silver atoms from very stable sites on the surface of the gold metal, results in the formation of a monolayer peak during a stripping scan.

From the data presented above, the amount of silver that is deposited on the ceric treated electrode surface at potentials more anodic than 0.30 volts, is less than for the crystalline surface. It is reasonable to expect that the same lesser number of atoms would be removed in the monolayer appearing after the reversible stripping peak. The area under the deposition and stripping current-time plots

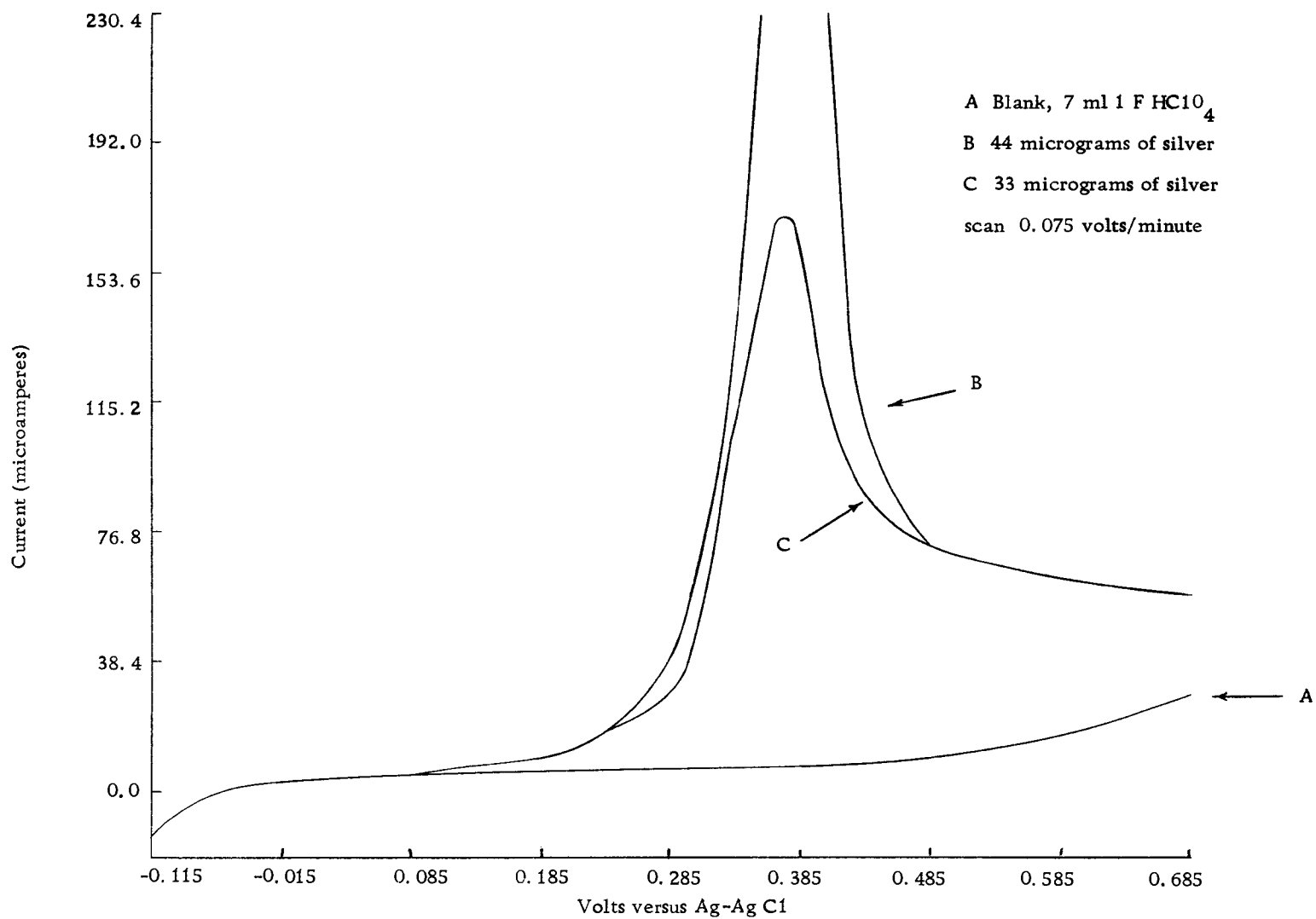


Figure 19. Stripping scans of silver from the ceric treated gold surface.

for the ceric treated gold surface agrees within experimental error.

During the study of deposition at ceric treated surfaces, several other electrode surface effects were observed. Figure 20 shows the deposition and stripping curves for 166 micrograms of silver at the crystalline gold electrode surface. The $w_{\frac{1}{2}}$ is much less than 0.0906 volts, but still greater than 0.0178 volts. The instrument used in this work could not deliver the currents necessary to deposit gross amounts of silver which would be required to have a $w_{\frac{1}{2}}$ of 0.0178 volts.

Figure 21 shows the data obtained when 154 micrograms of silver were deposited and stripped at the ceric treated gold surface. The interesting thing here is the double peaks that appear in the stripping scan. It was discovered that after many deposition and stripping scans were run, the double peaks would disappear, and one peak similar to that in Figure 20 would appear. If the electrode was given a ceric treatment, the double peaks would again appear. The double peaks suggest the possibility that the silver may be deposited in layers of different potential energies. A possible explanation for this is that one peak (second one on the stripping scan) could result from the oxidation of the silver atoms in the lower potential energy sites, such as the layer on the gold metal, and the silver required to fill all the holes and surface irregularities (edges and kinks) in the silver deposit. The first peak on the stripping scan could result

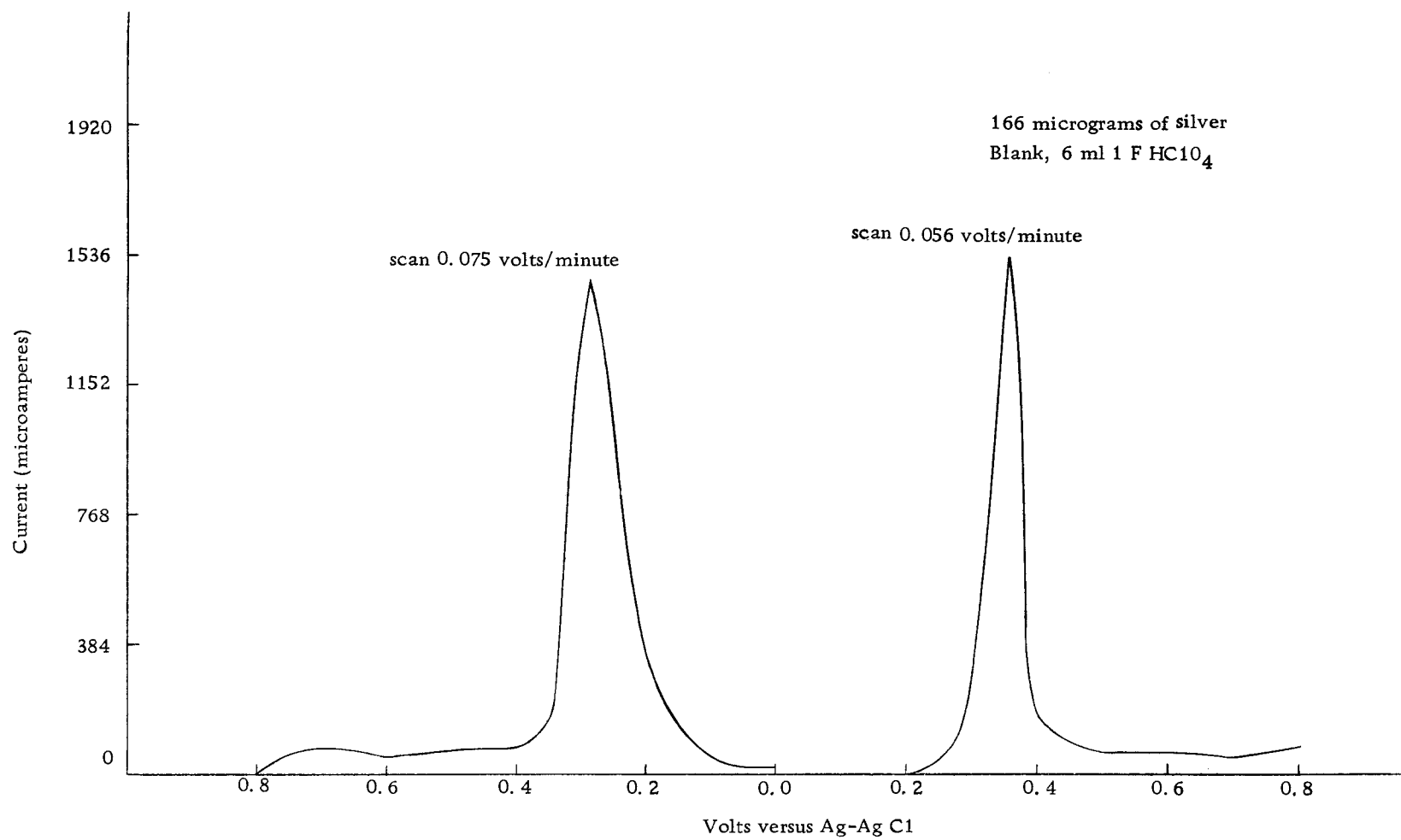


Figure 20. Deposition and stripping of silver at the crystalline gold surface.

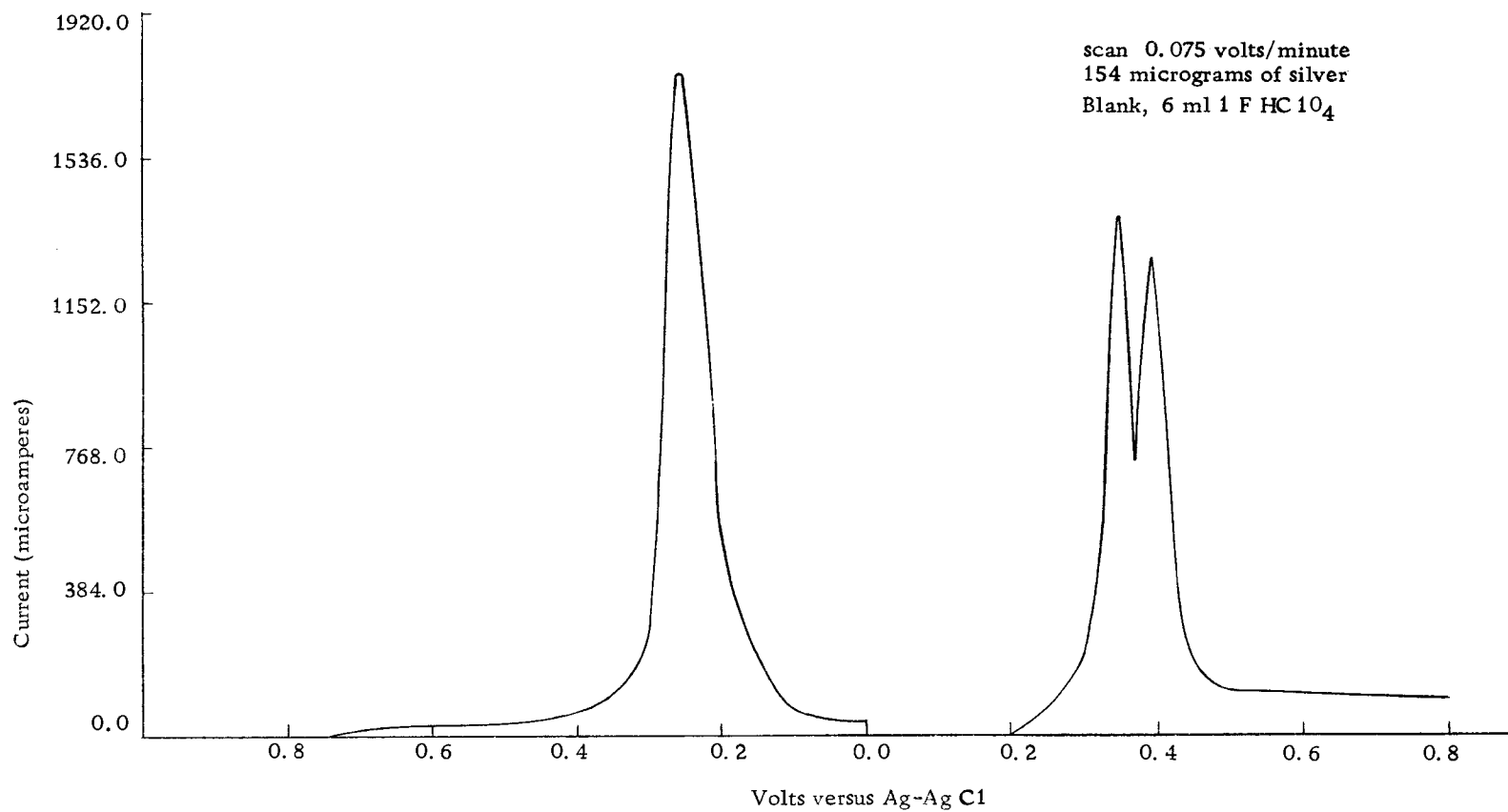


Figure 21. Deposition and stripping of silver at the ceric treated gold surface.

from the oxidation of silver from the smooth layers of silver deposited on silver. This layer would not have the high desorption energy barrier or the forces of attraction between gold and silver atoms that the first one or two silver layers would have. This seems to be a reasonable explanation, and by consulting Figure 20, it can be shown that the stripping peak for the crystalline electrode surface is within five millivolts of the first stripping peak on the ceric treated electrode. By consulting Figure 19, it can be seen that the potential for the current maximum of the second stripping peak is within 10 millivolts of the peak voltage for the stripping of small amounts of silver from the ceric treated gold surface. The amounts of silver removed from the electrode in Figure 19 is not enough to form the first of the double peaks shown in Figure 21. It can also be seen in Figures 20 and 21 that the deposition current maximum occurs at a more negative potential for the ceric treated electrode surface than that for the crystalline surface. This was observed previously for the deposition of smaller amounts of silver on the ceric treated gold surface. The fact that the double peaks disappear after many voltage scans might be explained in the following manner. The gold atoms on the surface of the electrode could migrate to more stable lattice sites, resulting in a more crystalline electrode surface. This was also observed in the study of iron.

Conway (9) discusses the surface migration of silver adions

and when one realizes that a gold atom on the surface of the electrode may have several water molecules in its coordination sphere, as well as several gold atoms, it is not difficult to expect the migration of gold atoms to more stable lattice sites which is similar to the migration of silver adions from a planar surface to a lattice vacancy.

A study was made also of silver deposition on a ceric treated platinum surface. The deposition and stripping current-time plots are shown in Figure 22. As can be seen, the area under the stripping curve is a small fraction of the area under the deposition plot. When a reduction and oxidation scan were run again on the same solution as that in Figure 22, the deposition curve appeared slightly larger than the stripping curve in Figure 22. The subsequent stripping curve was much smaller than the stripping curve in Figure 22. When this electrode was given a potassium iodide-sulfuric acid treatment to smooth it, the current-time plot shown in Figure 23 was obtained. Looking again at Figure 22, it can be seen that the potential of the reversible deposition peak has shifted in a negative direction as in the case of deposition on a ceric treated gold surface. Other deposition scans of silver on the ceric treated platinum surface showed that very little silver was deposited before the reversible peak appeared. This was similar to data obtained with the ceric treated gold electrode.

The above results can partially be explained in the following

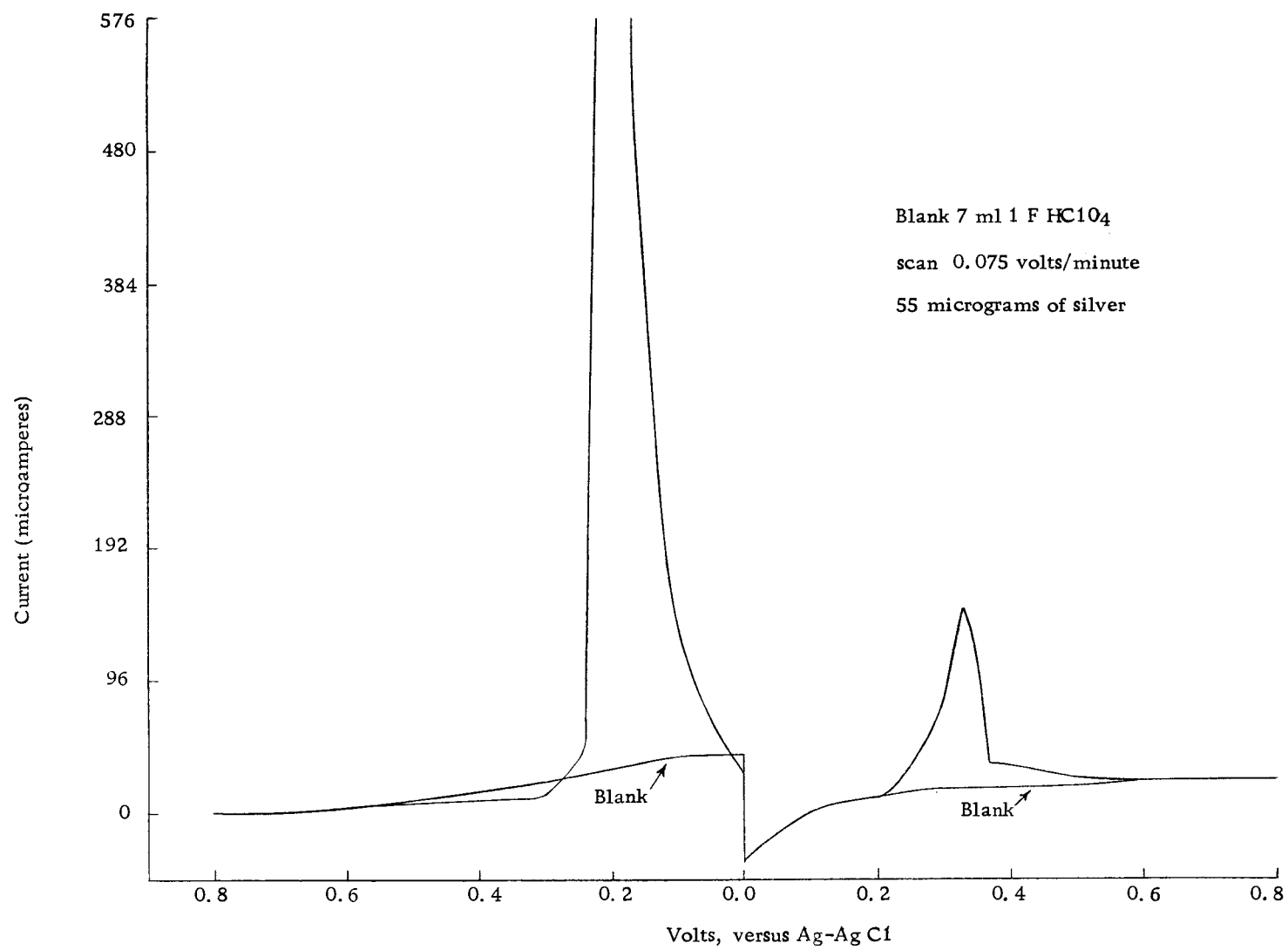


Figure 22. Deposition and stripping of silver at the ceric treated platinum electrode.

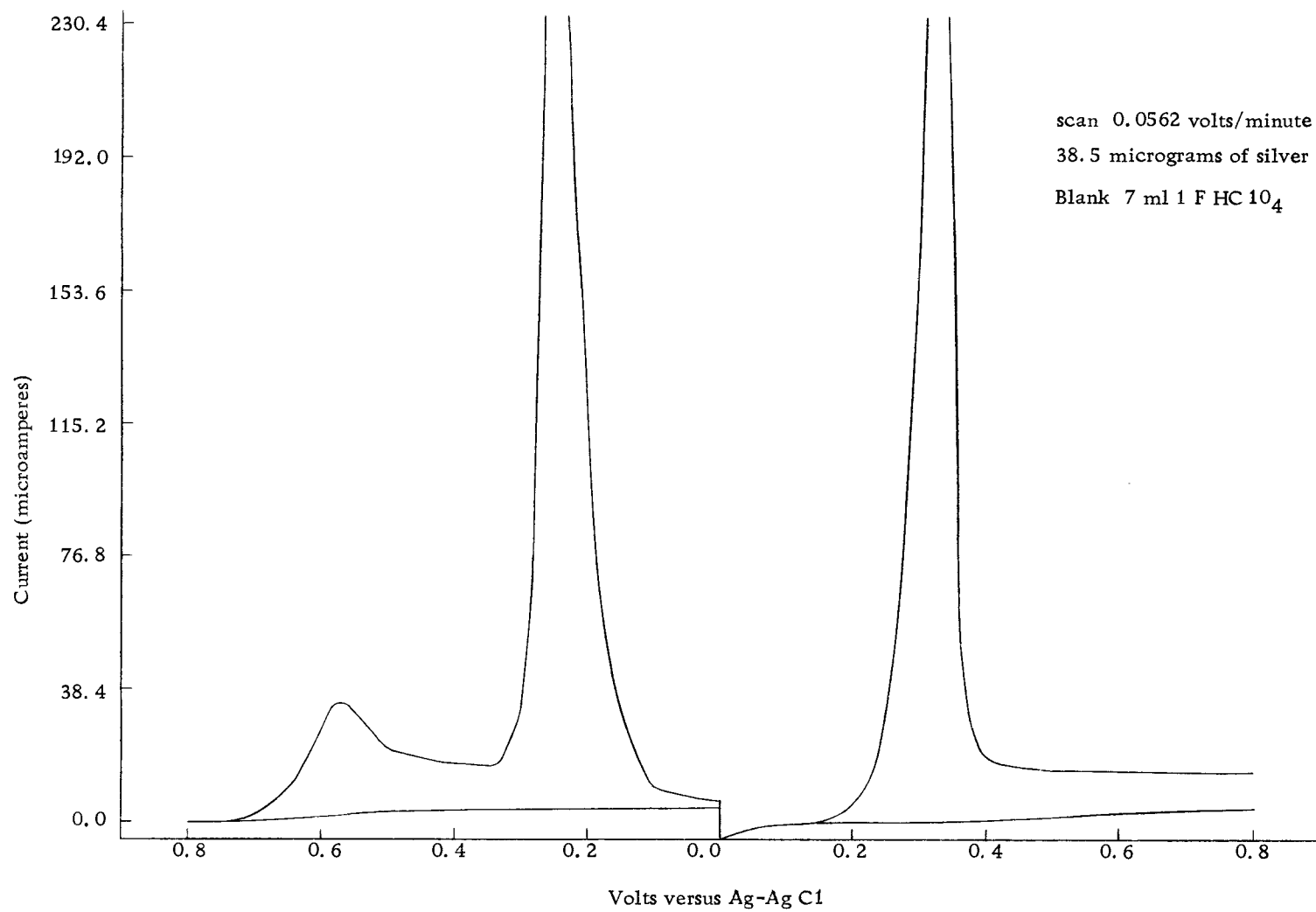


Figure 23. Deposition and stripping of silver at the crystalline platinum surface.

manner. If the ceric treated surface of the platinum electrode is somewhat amorphous, then it would be expected that the potential for the current maximum on the deposition scan would be shifted negatively as the data indicates. It is also possible that the silver atoms deposited in the bottom of holes and lattice vacancies on the platinum surface are not removed during an oxidation scan because they may be in extremely low energy sites. These silver atoms would also have a high desorption energy barrier. One possible reason this does not happen on the gold electrode can be partially explained by consulting Latimer (17, p. 197, 208). He lists the formal potentials for the reduction of Au^{+3} as 1.50 volts and the reduction of Pt^{+2} as about 1.20 volts versus the normal hydrogen electrode. These formal potentials indicate that gold is the more noble metal in regard to oxidation in an aqueous solution. It would seem reasonable to conclude that the platinum surface would show more extensive oxidation and roughening than the gold surface from the same oxidizing treatment.

Iodide-Iodine Couple

The iodide-iodine couple was studied briefly with voltage scanning coulometry. Figure 24 illustrates the current-voltage plot obtained for this couple. The curves in Figure 24 show the effect of different concentrations of potassium iodide and electrode surfaces

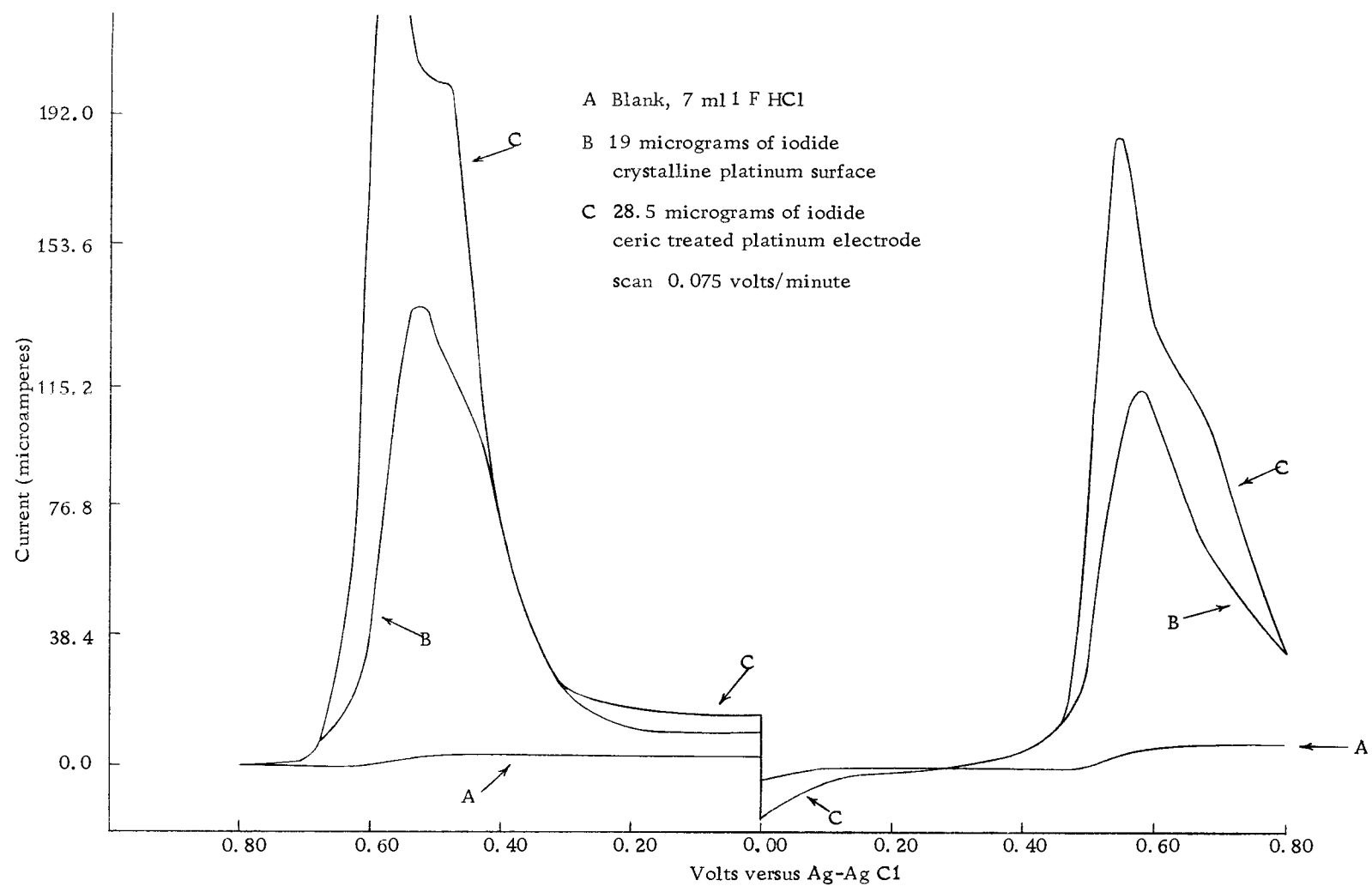


Figure 24. Oxidation and reduction scans of iodine at the platinum electrode.

on the current-voltage plots. The effect of the electrode surface on the electrochemistry of the iodide-iodine couple appears to be very minor. This is contrasted with the large effect of the electrode surface on the iron and silver systems, both previously discussed.

Peekema (22, p. 15) derived Equation 18 for the reduction of iodine. In order to check this equation, the working electrode must be corrected for polarization. The method used to correct the working electrode for polarization in the iron system should be applicable here, also. This was not attempted here, and the checking of the derived equations will be left for a future study.

Anson and co-workers (12, 21) have recently published extensive work on the iodide-iodine couple at platinum electrodes. Their results indicate that even though there is evidence for adsorption of iodide and iodine on the platinum electrode, the adsorption cannot be a significant part of the electron transfer mechanism. Their data also reveals that iodide is not adsorbed in an electroactive state on the surface of the electrode while iodine is adsorbed.

Since adsorption is apparently not part of the electron transfer mechanism, it is easy to understand why the electrode surface has little effect on the electrochemistry of the iodide-iodine couple. Since ferrous or ferric ions show electroactive adsorption on the electrode (2), it is reasonable to expect that the electrode surface would effect the electrochemistry of the iron system.

V. SUMMARY

Voltage scanning coulometry is used to study the effects of electrode treatments on subsequent electrode reactions. Quantitative verification of theoretical equations describing metal deposition and the ferric-ferrous couple is included.

The analytical technique called voltage scanning coulometry is very similar to controlled potential coulometry. The main difference is that the potential of the working electrode is scanned through a voltage range instead of remaining at a constant potential. The data obtained with this technique is normally a plot of current versus voltage or time.

The more important conclusions resulting from this work are listed below:

1. The theoretical equation describing the electrochemistry of a couple with both oxidized and reduced species present as ions in solution is verified for the ferric-ferrous couple.
2. The theoretical equation for submonolayer metal deposition based on the assumption that the activity of the deposit is related to the fraction of the electrode surface area covered by the deposit is verified for the stripping of silver from a gold electrode.
3. Experimental evidence for the presence of both gold and

platinum oxides is presented.

4. The effective to geometric surface area ratio is determined for silver deposition on a crystalline gold surface to be 2.3.
5. Qualitative evidence verifying the potential energy calculations for silver deposition is presented. The activity of submonolayer deposits of silver on a crystalline gold electrode is less than the corresponding activity on a crystalline platinum surface. The activity of the submonolayer deposit is much larger for silver deposition on either a ceric treated gold or platinum surface than on a crystalline gold or platinum surface.
6. Evidence showing that a ceric treated electrode surface catalyzes the reduction and oxidation of the ferric-ferrous couple at the gold electrode.
7. The first silver monolayer is deposited around three adsorption energies on the crystalline gold electrode. For deposition at the ceric treated gold surface there were no discrete adsorption energies.

BIBLIOGRAPHY

1. Anson, Fred C. Effect of surface oxidation on the behavior of platinum electrodes. *Analytical Chemistry* 33:934-939. 1961.
2. Anson, Fred C. Chronopotentiometry of iron (II) and iron (III) adsorbed on platinum electrodes. *Analytical Chemistry* 33:1498-1502. 1961.
3. Anson, Fred C. and James J. Lingane. Chemical evidence for oxide films on platinum electrometric electrodes. *Journal of the American Chemical Society* 79:4901-4904. 1957.
4. Baxter, R. A. and C. G. Enke. A versatile and inexpensive controlled potential polarographic analyzer. *Journal of Chemical Education* 41:202-209. 1964.
5. Bockris, J. O'M. and B. E. Conway (eds.) Modern aspects of electrochemistry. No. 3. London, Butterworths, 1964. 455 p.
6. Bockris, J. O'M. and D. B. Mathews. The mechanism of charge transfer at electrodes. *Journal of Electroanalytical Chemistry* 9:325-327. 1965.
7. Bowden, F. P. and E. K. Rideal. On the electrolytic behavior of thin films. Part II. The areas of catalytically active surfaces. *Proceedings of the Royal Society of London, Ser. A*, 120:80-89. 1928.
8. Bryne, J. T., L. B. Rogers and J. C. Greiss, Jr. Electrodeposition behavior of traces of silver. III. Transition region between "trace" and "macro" behavior. *Journal of the Electrochemical Society* 98:452-463. 1951.
9. Conway, B. E. and J. O'M. Bockris. On the calculations of potential energy profile diagrams for processes in electrolytic metal deposition. *Electrochimica Acta* 3:340-366. 1961.
10. Greiss, J. C., Jr., J. T. Bryne and L. B. Rogers. Electrodeposition behavior of traces of silver. II. Effects of electrode history and the presence of other ions. *Journal of the Electrochemical Society* 98:447-451. 1951.

11. Hubbard, Arthur T. and Fred C. Anson. Linear potential sweep voltammetry in thin layers of solution. *Analytical Chemistry* 38:59-61. 1966.
12. Hubbard, Arthur T., Robert A. Osteryoung and Fred C. Anson. Further study of the iodide-iodine couple at platinum electrodes by thin layer electrochemistry. *Analytical Chemistry* 38:692-697. 1966.
13. Hush, N. S. Adiabatic rate processes at electrodes. I. Energy-charge relationships. *The Journal of Chemical Physics* 28:962-972. 1958.
14. Kolthoff, I. M. and James J. Lingane. *Polarography*. 2d ed. Vol. 1. New York, Interscience Publishers, 1952. 420 p.
15. Laitinen, Herbert A. *Chemical analysis*. New York, McGraw-Hill, 1960. 611 p.
16. Laitinen, H. A. Electroanalytical chemistry of surface monolayers. *Analytical Chemistry* 33:1458-1464. 1961.
17. Latimer, W. M. *The oxidation states of the elements and their potentials in aqueous solutions*. New York, Prentice-Hall, 1952. 392 p.
18. Lingane, James J. *Electroanalytical chemistry*. 2d ed. New York, Interscience Publishers, 1958. 669 p.
19. Malmstadt, H. V., C. G. Enke and E. C. Toren, Jr. *Electronics for scientists*. New York, W. A. Benjamin, 1963. 619 p.
20. Meites, Louis and Steven A. Moros. Background corrections in controlled-potential coulometric analysis. *Analytical Chemistry* 31:23-28. 1959.
21. Osteryoung, R. A. and F. C. Anson. Behavior of the iodide-iodine couple at platinum electrodes. *Analytical Chemistry* 36:975-980. 1964.
22. Peekema, Richard M. *Voltage scanning coulometry*. Ph. D. thesis. Pullman, Washington State University, 1962. 99 numb. leaves.

23. Peekema, Richard M., IBM Corp., Neighborhood Road, Kingston, New York. Personal communication. June 15, 1966.
24. Rogers, B. A. The nature of metals. Ames, Iowa State College Press, 1951. 248 p.
25. Rogers, L. B. and A. F. Stehney. The electrodeposition behavior of a simple ion. Transactions of the Electrochemical Society 95:25-32. 1949.
26. Rogers, L. B., D. P. Krause, J. C. Griess and D. B. Ehrlinger. The electrodeposition behavior of traces of silver. Transactions of the Electrochemical Society 95:33-46. 1949.
27. Schmidt, P. P. Jr., and H. B. Mark, Jr. Quantum chemistry of electrode processes. I. General relations for electron exchange between electrode and electroactive species under equilibrium and nonequilibrium conditions. The Journal of Chemical Physics 43:3291-3299. 1965.
28. Scott, R. A., R. M. Peekema and R. E. Connally. Voltage scanning coulometry for the determination of traces of iron. Analytical Chemistry 33:1024-1027. 1961.
29. Strobel, Howard A. Chemical instrumentation. Reading, Mass., Addison-Wesley, 1960. 653 p.
30. Vines, R. F. The platinum metals and their alloys. New York, International Nickel Company, 1941. 141 p.
31. Yeager, Ernest (ed.) Transactions of the Symposium on Electrode Processes, Philadelphia, 1959. New York, Wiley, 1961. 374 p.